NASA TN D-310

TECHNICAL NOTE
D-310

TESTS OF AN AREA SUCTION FLAP ON AN NACA 64A010 AIRFOIL AT HIGH SUBSONIC SPEEDS

By Donald W. Smith and John H. Walker

Ames Research Center
Moffett Field, Calif.

NATIONAL AERONAUTICS AND SPACE ADMINISTRATION
WASHINGTON

May 1960

1R

NATIONAL AERONAUTICS AND SPACE ADMINISTRATION

TECHNICAL NOTE D-310

TESTS OF AN AREA SUCTION FLAP ON AN NACA 64A010 AIRFOIL AT HIGH SUBSONIC SPEEDS

By Donald W. Smith and John H. Walker

SUMMARY

The lift, drag, chordwise distribution of static pressure and boundary-layer velocity profile at 0.85c were measured for a two-dimensional wing with an NACA 64A010 airfoil section. The wing had a plain flap with a chord of 0.30 of the wing chord. The perforated suction area was variable and extended from 0.69 to 0.90 of the wing chord. Data were obtained for several different suction-area configurations at a Reynolds number of 2.9×10^6 for a range of Mach numbers from 0.70 to 0.84.

A reduction of the section drag coefficient for a constant section lift coefficient was obtained by application of suction over the area from 69 to 72.5 percent of the wing chord. The largest reduction was obtained for the model with less than 2° flap deflection at Mach numbers of 0.80 and 0.82 for lift coefficients above about 0.35. However, for the highest lift coefficients at the test Mach numbers of 0.80 and 0.82, nearly the same drag reduction was obtained with the flap deflected 6° without suction.

The ability of the area suction to control the boundary layer was not affected by the trip wire on the forward part of the wing which was used to induce transition artificially.

INTRODUCTION

Reference 1 summarizes previous investigations of boundary-layer suction and presents data for airfoils with suction at various locations. No improvements in high-speed drag characteristics were found. Studies of airfoils with plain flaps (e.g., NACA TN 3174) have shown that some improvements of drag at high subsonic speeds are obtained at moderate and large lift coefficients by the use of small flap deflections.

The present investigation was undertaken to study the possibility of preventing shock-induced separation on a wing with a plain flap through the use of area suction, and hence of reducing the drag of the wing. It was thought that the deflected flap would maintain the shock wave in the region of the suction area, causing the point of minimum pressure to occur

at the hinge line and the pressure recovery through the shock to occur on the flap while both Mach number and angle of attack were varied. Area suction was applied over the forward portion of the flap where shock-induced separation should occur. If sufficient suction were applied to prevent separation then a reduction in drag should result.

NOTATION

c wing chord, ft

c_d section drag coefficient

c_l section lift coefficient

c_Q section flow coefficient through the porous area

C_p pressure coefficient, $\frac{p-p_\infty}{q_\infty}$

M_l local Mach number

M_∞ free-stream Mach number

p local static pressure, lb/sq in.

p_∞ free-stream static pressure, lb/sq in.

q_∞ free-stream dynamic pressure, lb/sq in.

x chordwise distance from wing leading edge in the direction of the flow

y vertical distance from the surface of the wing

α angle of attack, deg

δ flap deflection, deg

MODEL AND APPARATUS

Model

The model used in the investigation had an NACA 64A010 airfoil section and a constant chord of 20 inches and completely spanned the test section of the Ames 12-foot pressure wind tunnel. Because of its extreme span-to-chord ratio, the airfoil was restrained from bending due to lift by a tie rod that extended from the airfoil midspan to the tunnel wall. The model was equipped with a plain flap with a chord 0.30 of the airfoil chord. The flap was hinged at the lower surface and was capable of being deflected from 0° to 10° in 1° increments. Provisions were made for applying distributed suction on the upper surface of the flap. A photograph of the model in the wind tunnel is shown in figure 1 and sketches of the model are presented in figure 2.

The portion of the airfoil ahead of the flap was constructed to provide an air duct within the airfoil, for removing air from the perforated flap. Turning vanes and a flow-regulator bar oriented spanwise were arranged in the duct to provide a uniform spanwise distribution of flow through the perforated surface when suction was applied (see fig. 2(b)). Bench tests established the appropriate arrangement of the turning vanes and the regulator bar. A plenum chamber was provided in the flap to facilitate removal of boundary-layer air through the perforated upper surface. The surface was constructed of a 0.030-inch-thick stainless steel sheet which had 179 holes per square inch. The holes were 0.040 inch in diameter and were arranged in a staggered pattern. This material provided a surface which was 23 percent open. The perforated area extended from 0.69 to 0.90 of the airfoil chord. Variation of the chordwise extent of the perforated area was obtained by sealing portions of the perforated sheet with cotton aircraft tape which was coated with aircraft dope and sanded to have a smooth, nonporous finish. Five pressure orifices were distributed spanwise along the plenum chamber to measure plenum chamber pressure. For a few tests the flap was fitted with a solid aluminum upper surface which replaced the perforated sheet.

The flap hinge was sealed to prevent flow of air from the lower surface into the flap plenum chamber. The gap between the airfoil upper skin and the upper surface of the flap was also sealed so that air could be drawn only through the perforated area.

Four chordwise rows of static-pressure orifices were located 16 and 49 inches either side of the airfoil midspan (fig. 2(a)). Orifices were provided on both the upper and lower surfaces of the airfoil.

Two fences were mounted on the airfoil 5 inches from each tunnel wall as shown in figures 1 and 2(a). The fences were provided in an attempt to minimize the effect of the tunnel boundary layer on the air flow over the model.

For a limited number of tests a boundary-layer trip was installed on the upper surface of the wing at 20 percent of the airfoil chord. The trip consisted of an 0.008-inch-diameter steel wire cemented to the airfoil surface from one end fence to the other.

Apparatus

The wind-tunnel balance system was used for measuring the model lift and drag.

The air drawn through the perforated flap was removed from each end of the airfoil through 8-inch-diameter pipes by a vacuum pump located outside the wind tunnel. A mercury seal was installed in the suction line to provide a frictionless coupling between the balance system and the pipe fixed to the wind tunnel. The air flow quantity through the suction lines was measured with standard ASME square-edge orifice meters. During the entire test, a boundary-layer rake was mounted on the upper surface of the flap at 0.85 x/c (see figs. 1 and 2(a)).

TESTS AND PROCEDURE

Tests

The operating conditions for each model configuration investigated are given in table I. The test procedure used with all configurations was to set a constant Mach number and to vary the quantity of air flow through the perforated area for each angle of attack. Each test run was started with the maximum amount of air flow, usually a c_Q of about 0.002, and then data were recorded for reduced amounts of suction flow until a final reading with no air flow was taken.

Reduction of Data

The test data have been reduced to standard coefficient form. Factors which affect the accuracy of these results and the corrections applied are discussed in the following paragraphs.

Tunnel-wall interference.- The data have been corrected for the influence of the tunnel walls by the method of reference 2. At a Mach number of 0.80 the corrections to the drag coefficient and the lift coefficient were 1.4 and 2.3 percent, respectively. At a Mach number of 0.80 the correction to Mach number amounted to a 1/2-percent increase over that determined from a calibration of the tunnel without a model in place.

Stream variations.- In the test region, the stream inclination was less than 0.08°. This was determined from a tunnel calibration with a wing spanning the tunnel at 0° angle of attack. The longitudinal variation of the static pressure in the region of the model was less than 0.2 percent of the dynamic pressure. No correction for the effect of these variations was made.

Two-dimensionality of flow over the airfoil.- Although the airfoil was carefully constructed, it had a small permanent spanwise twist amounting to about 0.25°. The airfoil being very limber was also capable of twisting under load because it was fixed in torsion only at its ends. Despite these two factors, comparison of the chordwise distribution of static pressure at the various spanwise stations did not reveal any major variations across the span.

Suction quantity.- The equations for square-edge orifice meters given in reference 3 were used to compute the weight flow of air removed from the boundary layer through the perforated area.

Drag.- The measured drag of the wing was corrected to account for the power required to pump the sucked air downstream, through a suitable nozzle, in the free-stream direction. Therefore, the drag coefficients presented in the report are effective drag coefficients if 100-percent pump efficiency and no duct losses are assumed:

$$c_d = c_{d_{measured}} - 2c_Q + c_{pump}$$

For additional information regarding this correction see reference 4 (p. 39) and reference 5. The pumping drag coefficient was computed by the method given in appendix III of reference 1. The value of the drag coefficient equivalent to the pumping power had a maximum value of about 0.005.

The gross drag of the wing was corrected for turntable tares but no correction was made for the drag of the fences, the drag of the boundary-layer rake, or the drag of the streamlined tie wire at the center of the wing. However, at a constant Mach number these drag contributions would probably be relatively unaffected by flap deflection or by the application of the area suction, and hence would not mask the effectiveness of suction in changing the drag. At a Mach number of 0.80, the drag coefficient of the tie rod in terms of the wing area was estimated to be about 0.0048; it was expected that the drag of the fences, being mainly skin friction, would be quite small when expressed in terms of the wing area. No estimate was made of the drag of the rake. In summary, the drag coefficient values presented include the drag of the tie rod, fences, and rake, and can only be used to determine drag increments produced by suction or flap deflection.

An attempt was made to determine the pressure drag of the airfoil by spanwise integration of the local pressure drag at the four spanwise orifice stations. These values of pressure drag were considered of doubtful accuracy because of uncertainty in the spanwise variation of pressure drag between the outboard orifice stations and the tunnel walls.

RESULTS AND DISCUSSION

Data are presented in figures 3, 4, and 5 which show the effect of area suction on the airfoil section lift and drag coefficients, the chordwise distribution of static pressure, and the airfoil boundary-layer Mach number profile at 85-percent chord. These data are for the airfoil with the flap deflected 1°, suction applied to the upper flap surface from 69 to 72.5 percent of the airfoil chord, and for Mach numbers from 0.75 to 0.82. The static-pressure data presented are for the left-hand inboard orifice station while the boundary-layer profile data were obtained on the right-hand semispan. The effects of area suction displayed by these data are representative of those observed in the majority of the data.

Data similar to that presented in figures 3, 4, and 5 have been plotted to show the effect of the variation of the chordwise extent of perforated area on the airfoil section lift and drag coefficients, suction quantity, and the chordwise distribution of static pressure, and are presented in figures 6, 7, and 8, respectively. These data are for the airfoil with the flap deflected 1° at a Mach number of 0.80. The effects at this Mach number and with this flap deflection are representative of those at Mach numbers and flap deflections where gains due to area suction were observed.

Effects of Chordwise Extent of Suction Area

The five different extents of suction area on the flap over which suction was applied are given in table I. The areas marked (d) (0.69 to 0.80 x/c) and (e) in the table (0.80 to 0.85 x/c) were discarded because the maximum amount of suction flow quantity available during the test failed to produce any effect on the section lift and drag.

The data presented in figures 6 through 8 show that, of the three remaining suction areas tested, the one extending from 69- to 72.5-percent airfoil chord was the best. Suction over this area resulted in the lowest drag for a given lift coefficient with the lowest c_Q, and also resulted, generally, in the best pressure recovery aft of the hinge line and at the trailing edge. The remainder of the discussion therefore will deal with the data obtained for the airfoil with the suction area extending from 69 to 72.5 percent of the airfoil chord.

Effects of Application of Area Suction

The most pronounced effect of the application of area suction to the upper surface of the airfoil from 69- to 72.5-percent chord occurred at Mach numbers of 0.80 (fig. 3(c)) and 0.82 (fig.3(d)), and was characterized by sharp discontinuities in the variations of both lift and drag coefficients with c_Q. In order to examine this phenomenon the lift and drag data, along with the associated chordwise pressure distributions and boundary-layer profiles, will be considered in some detail.

At a Mach number of 0.80 the largest effect of the application of suction occurred at an angle of attack of 3° (fig. 3(c)). Less effect was shown at other angles of attack. The data are qualitatively representative of the data obtained at other test conditions and will be used for the purpose of discussion.

It can be seen in figure 3(c) that for $\alpha = 3^\circ$ a decrease of c_Q from point D to point C resulted in a small decrease in lift and drag. Inspection of figure 5(d) shows that for these conditions ($c_Q = 0.00068$ and 0.00049), the chordwise distribution of static pressure was little changed while the boundary-layer profile showed a change which was due in part to a change in the local Mach number at the outer edge of the boundary layer. From point C to point B in figure 3(c) there was a sharp decrease of both lift and drag with an attendant increase in c_Q. Inspection of figure 5(d) shows that from point C to point B ($c_Q = 0.00049$ and 0.00071), there was a drastic change in both the pressure distribution and the boundary-layer profile. It appears that the boundary layer became thicker with separation probably being present in both cases. The minimum pressure point was moved forward from the hinge line and the pressure recovery near the trailing edge was not as good for point B. Change of c_Q from point B to point A resulted in only small changes in lift, drag, pressure distribution, and boundary-layer profile.

Application of area suction to the airfoil at Mach numbers of 0.75 (fig. 3(a)) and 0.78 (fig. 3(b)) resulted in small increases in section lift and drag coefficients with increase in c_Q. For a Mach number of 0.78 the chordwise pressure distribution and the boundary-layer velocity profiles (fig. 4) also show only gradual changes with increase in c_Q. The boundary-layer profiles indicate that boundary-layer separation occurred on the upper surface of the airfoil at this Mach number for angles of attack of 3° and 4°. Application of area suction seemed to have little effect on the separated boundary layer although the effect on the airfoil static pressures ahead of the suction area was pronounced.

Presented in figure 9 are the chordwise distribution of static pressure both with and without suction for several Mach numbers at angles of attack of $1/2^\circ$ and 2°. These pressure distributions along with those presented in figures 4 and 5 indicate that, at Mach numbers of 0.75 and 0.78, the

position on the airfoil of the minimum pressure (0.4c to 0.5c) and probably the origin of separation were too far forward for either improvement of the pressure recovery over the rear part of the airfoil or for control of the separation by application of area suction at the hinge line. However, at Mach numbers of 0.80 and 0.82 the minimum pressure occurred at about 60 percent of the airfoil chord and the application of suction at the hinge line resulted in marked changes in both the boundary-layer profiles and the pressure recovery over the rear of the airfoil. At the higher Mach numbers, application of suction also resulted in movement of the minimum pressure to the suction area. An exception to the above statements is shown by the data for a Mach number of 0.80 and an angle of attack of 4°: the minimum pressure point was far forward and application of suction resulted in no appreciable change in the flow over the airfoil.

The effects of area suction on the variation of section drag coefficient, at various constant section lift coefficients, with change of flap deflection and Mach number are presented in figures 10 and 11, respectively. In these figures are presented the airfoil data for both the flap with the solid aluminum upper surface (flap sealed) and the flap with suction applied to the perforated area extending from 69- to 72.5-percent airfoil chord. The suction data are presented for a suction quantity coefficient of 0.0006 both below (fig. 3(c) line AB) and above (fig. 3(c) line CD) the break in the curves of the variation of lift and drag with suction quantity discussed previously. For those curves without a break, only the point found on line AB was plotted.

The curves of figure 10 show that the drag was reduced appreciably below that for the flap-sealed value only when boundary-layer separation was reduced or prevented by application of suction. Drag reductions were realized at Mach numbers of 0.80 and 0.82 but only for the lowest flap deflections at section lift coefficients greater than about 0.35. Reductions of the same magnitude were obtained without suction at the highest lift coefficient by simply increasing the flap deflection to 6°, as can be seen in figure 10.

In figure 11 it can be seen that no appreciable increase of the drag rise Mach number was obtained by application of area suction to the airfoil upper surface.

Effect of Fixing Transition

The effects of fixing transition with a wire attached to the upper surface of the airfoil will be discussed for a Mach number of 0.80, with suction applied from 0.69c to 0.725c, and with a flap deflection of 3°. These data are representative of the data at other flap deflections and are presented because they are more complete than those available for other flap deflections.

Location of the transition point on the upper surface of the airfoil was determined for a few test conditions by visual flow studies employing the sublimation technique. These studies were made on only a small spanwise portion of the model but it was assumed that they applied over the major portion of the span. It was found that when the trip wire was used, transition occurred at the wire ($x/c = 0.20$), but when transition occurred naturally, it usually occurred just ahead of the hinge line.

In figures 12(a) and 13 are presented the free transition data. In figures 12(b) and 14 the data obtained with the trip wire are presented along with the faired curves for the free-transition data.

A
1
9
7

Application of suction in both cases resulted in an abrupt increase of lift and drag of about the same amount as shown in figure 12(b). However, the suction quantity required was somewhat smaller in the case of free transition.

The chordwise distribution of static pressure and the boundary-layer profiles were somewhat different for the two cases with zero suction. However, when suction was applied the static-pressure distributions became almost identical, and it was apparent that the boundary layer in both cases was made thinner if not completely unseparated.

CONCLUDING REMARKS

Several remarks may be made regarding the use of area suction on an airfoil to eliminate shock-induced separation.

At Mach numbers of 0.80 and 0.82, application of area suction at the hinge line of an airfoil with small flap deflections resulted in a reduction of the section drag coefficient at lift coefficients above about 0.35. However, even without suction, the drag at the highest lift coefficients was reduced by simply deflecting the flap. Deflection of the flap to an angle of 6° reduced the drag as much as the best area suction arrangement.

The ability of the area suction to control the boundary layer was not affected by the trip wire used on the forward part of the model to induce transition artificially.

Ames Research Center
National Aeronautics and Space Administration
Moffett Field, Calif., Dec. 18, 1959

REFERENCES

1. Leadon, B. M., and Anderson, G. E.: Boundary Layer Control on 64A006 and 64A010 Airfoils at High Subsonic Speeds. WADC Technical Report 53-490, 1953.

2. Vincenti, Walter G., and Graham, Donald J.: The Effect of Wall Interference Upon the Aerodynamic Characteristics of an Airfoil Spanning a Closed-Throat Circular Wind Tunnel. NACA Rep 849, 1946.

3. Anon.: Power Test Codes 1949. Supplement on Instruments and Apparatus, pt. 5. Measurement of Quantity of Materials. Ch. 4, sec. III.

4. Hoerner, Sighard F.: Aerodynamic Drag, 1951. The Otterbein Press, Dayton, Ohio.

5. Schrenk, O.: Experiments With Suction-Type Wings. NACA TM 773, 1935.

TABLE I.- TEST CONDITIONS AND MODEL CONFIGURATIONS

M	δ, deg					
	0	1	2	3	6	10
(a) Clean wing						
0.70	a	a	a	a	a	a
.75	abc	abc	ab	abc	acd	a
.78	abc	abcf	ab	abc	ac	a
.80	abc	abcf	ab	abc	acd	ac
.82	abc	abc	a	abd	acde	ac
.84	a	a	a	a	-	a
(b) Boundary-layer trip at 0.2 x/c						
.70	a	a	a	a	-	-
.75	a	a	ab	ab	c	-
.78	a	a	a	ab	-	-
.80	a	a	ab	ab	c	-
.82	a	a	a	ab	-	-
.84	a	a	a	a	-	-

Chordwise extent of porous area:

a. Plain Flap
b. 0.69 to 0.725 x/c
c. 0.69 to 0.75 x/c
d. 0.69 to 0.80 x/c
e. 0.80 to 0.85 x/c
f. 0.69 to 0.706 x/c

Notes:

1. $R = 2.9 \times 10^6$
2. α varied from -1° to 4° depending on δ and M.
3. Suction quantity for each configuration was varied from maximum to 0.

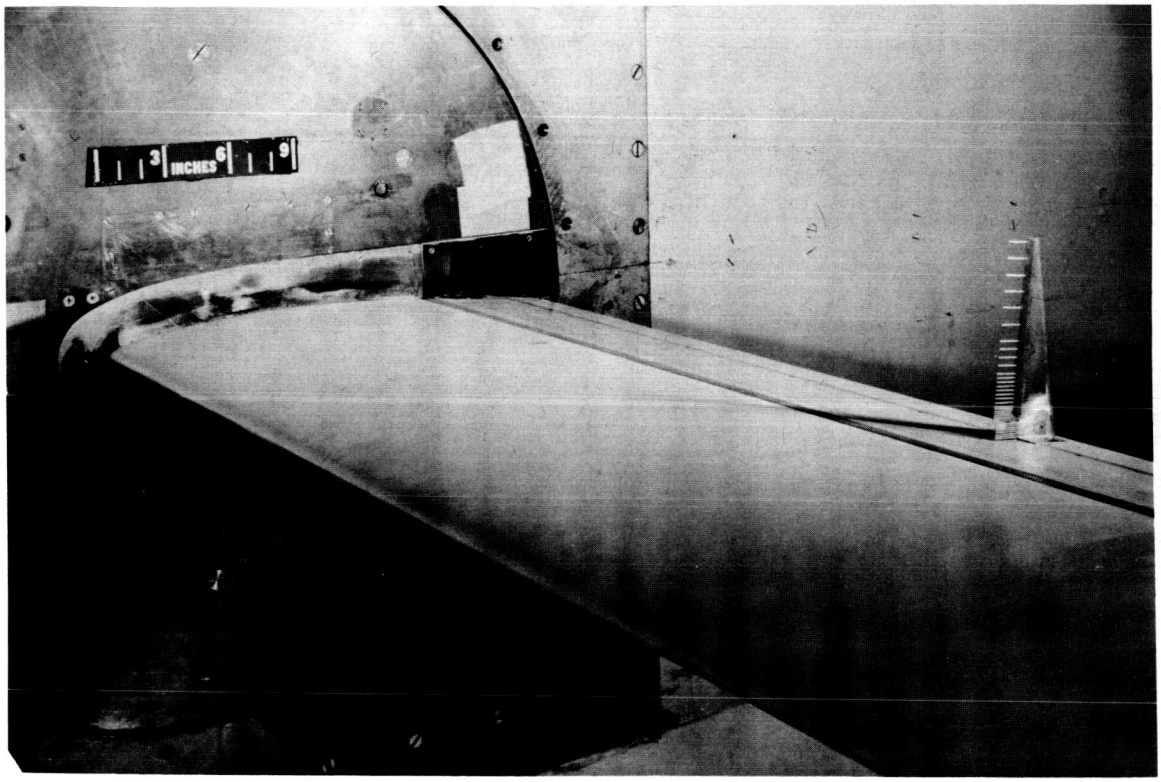

A-23738

Figure 1.- Photograph of the model in the test section of the Ames 12-foot pressure wind tunnel.

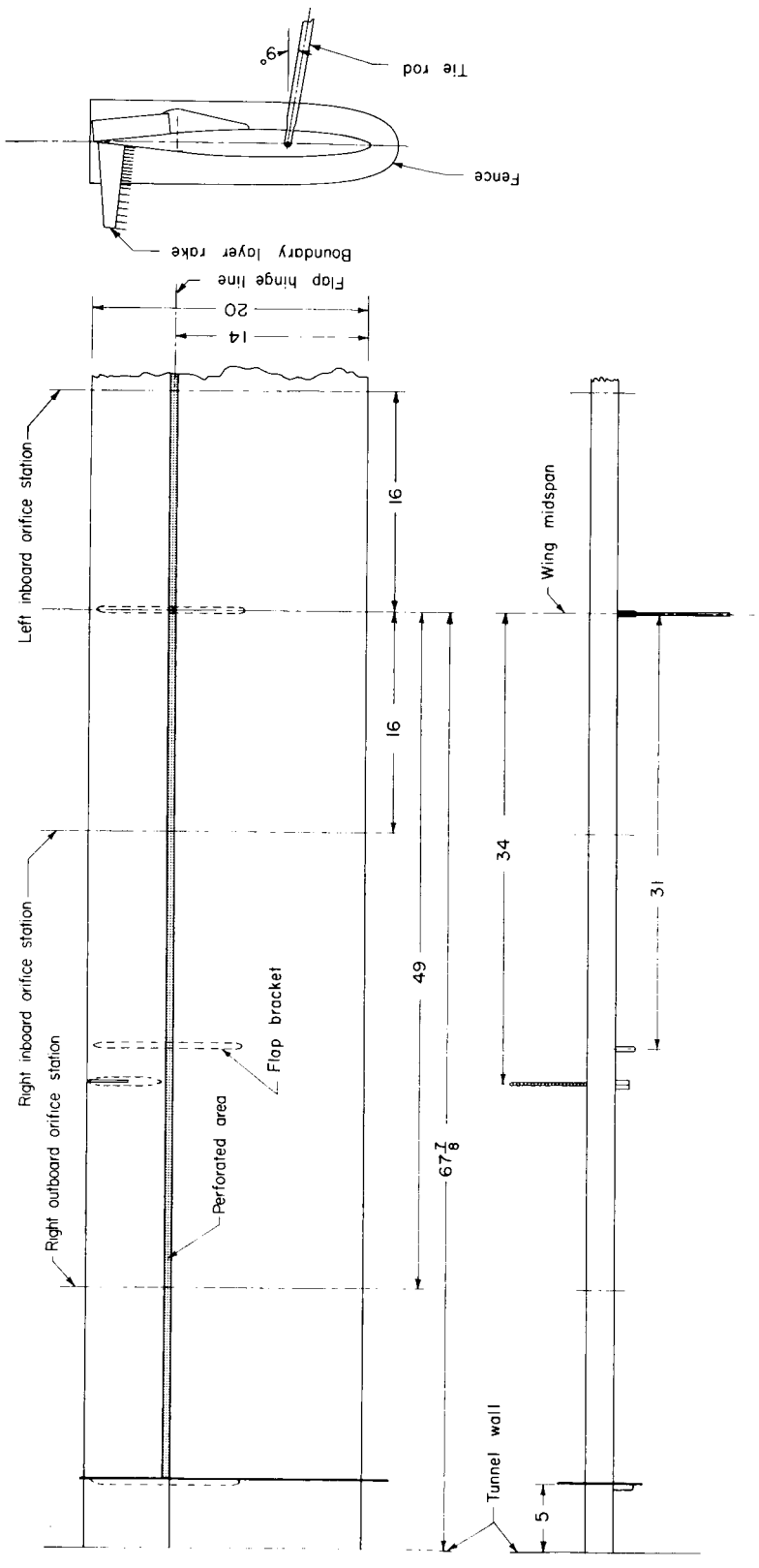

(a) Three-view drawing.

Figure 2.- Drawings of the model.

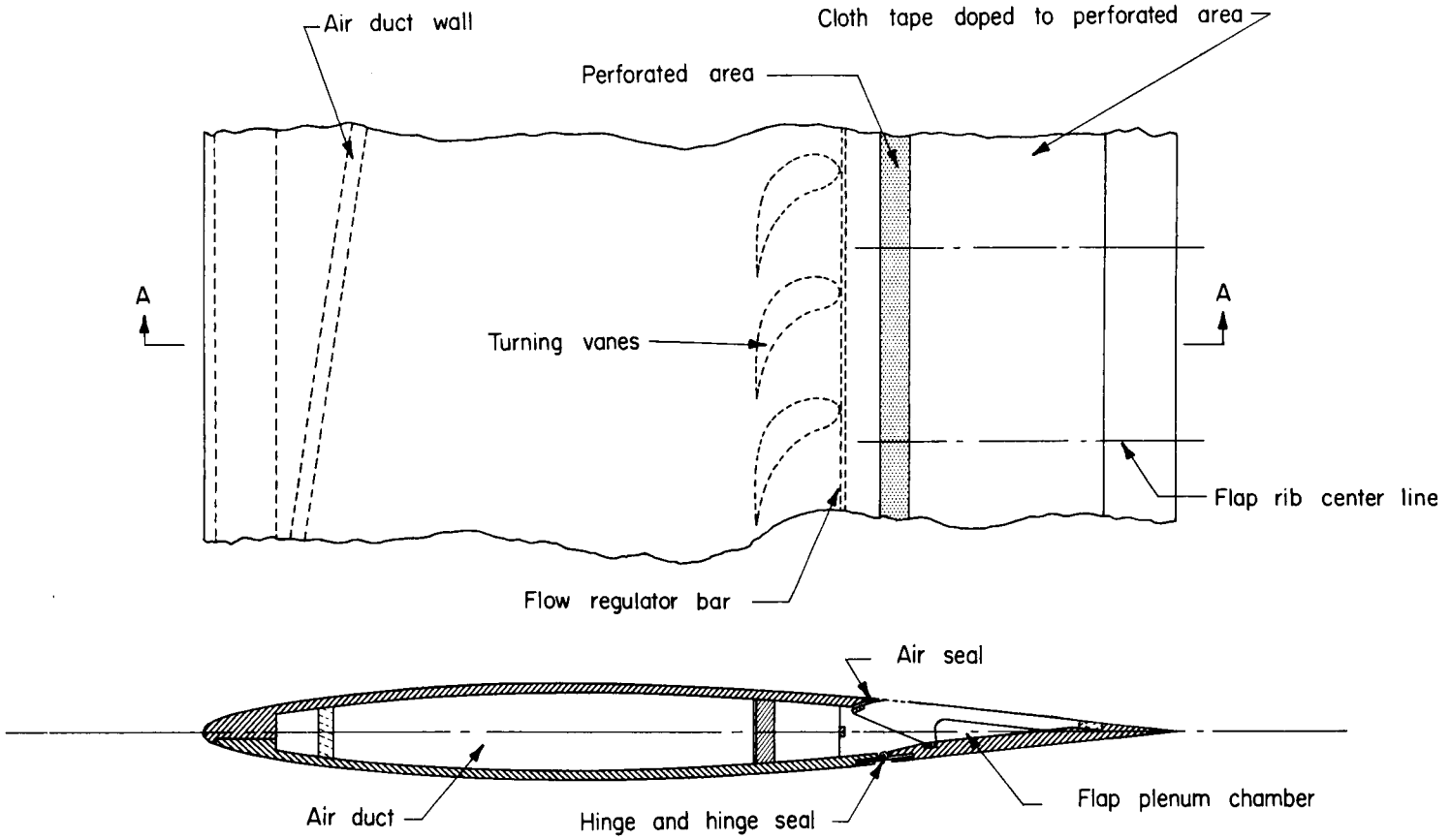

Section A-A

(b) Details of air duct.

Figure 2.- Concluded.

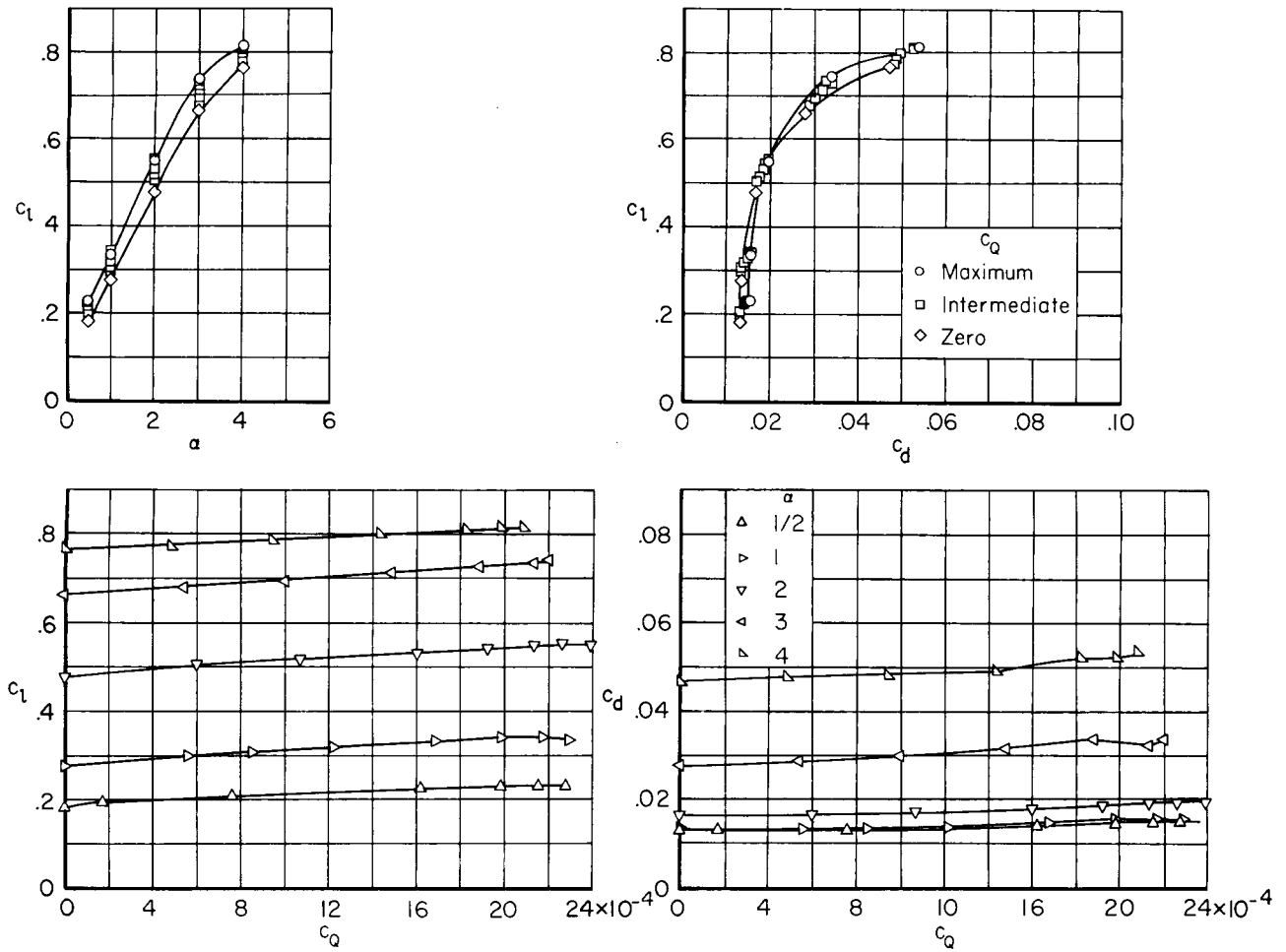

(a) $M_\infty = 0.75$

Figure 3.- Effect of suction quantity on section lift and drag coefficient; suction area extending from 0.69c to 0.725c; $\delta = 1^\circ$.

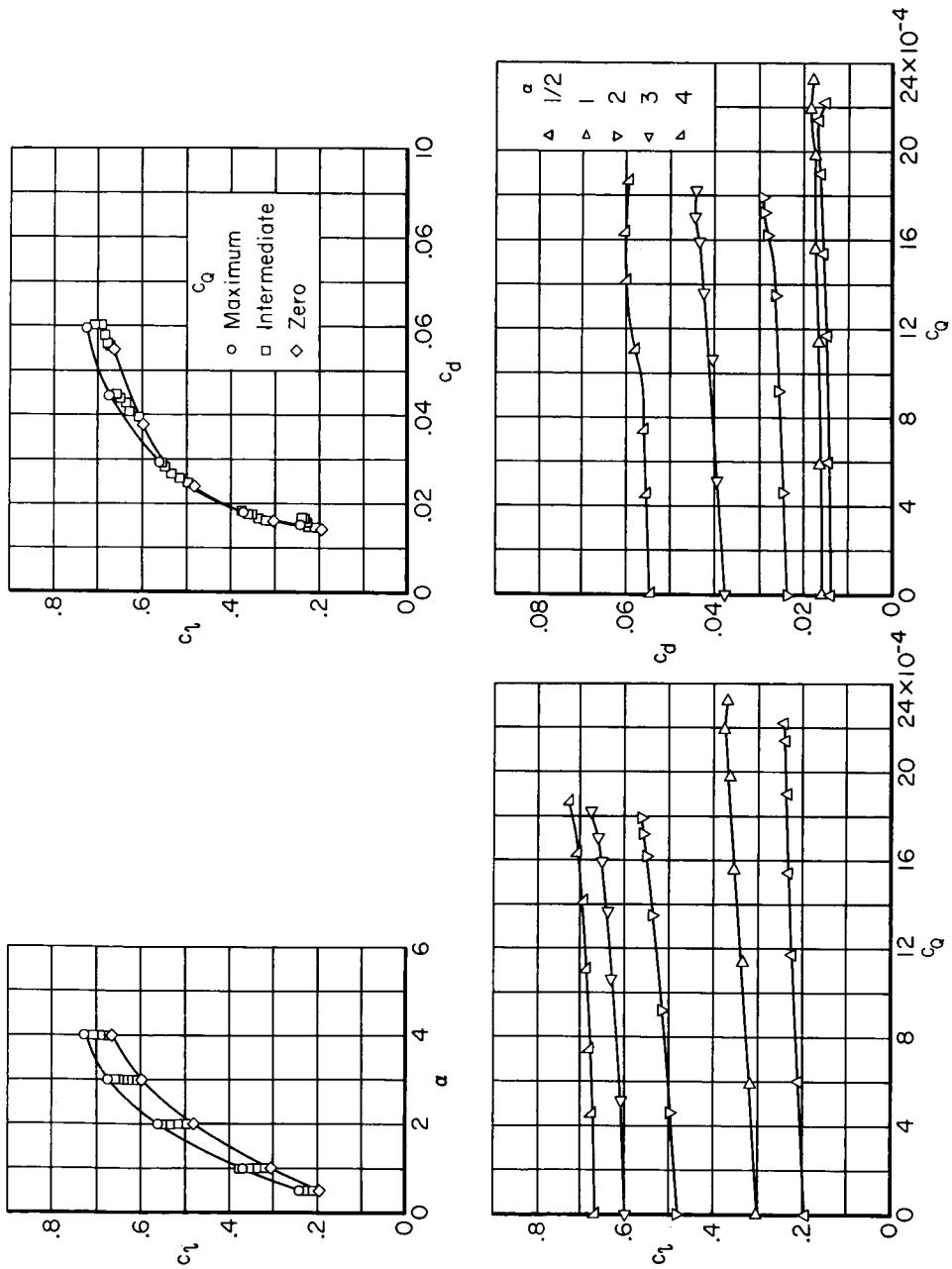

(b) $M_\infty = 0.78$

Figure 3.- Continued.

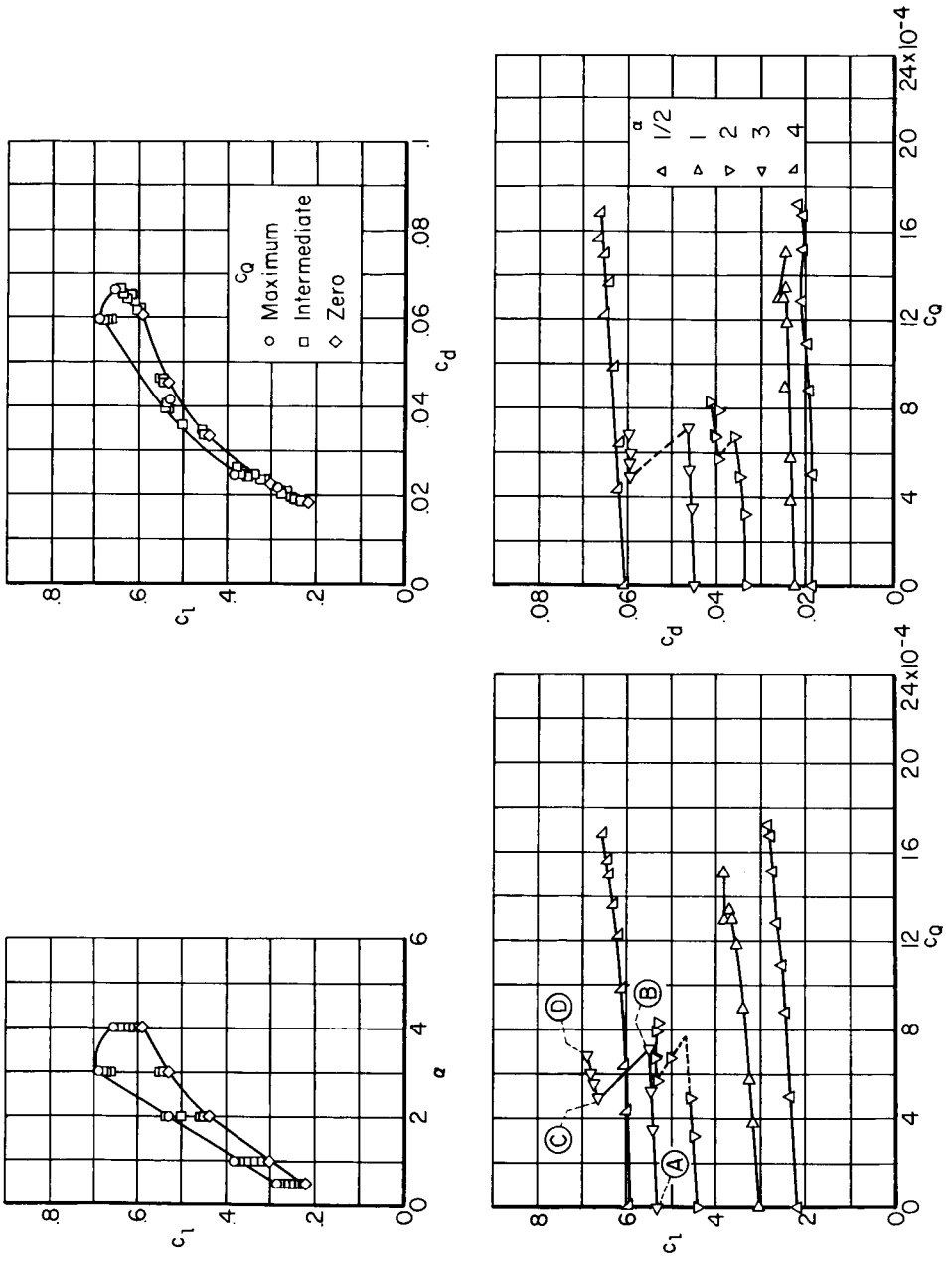

(c) $M_\infty = 0.80$

Figure 3.- Continued.

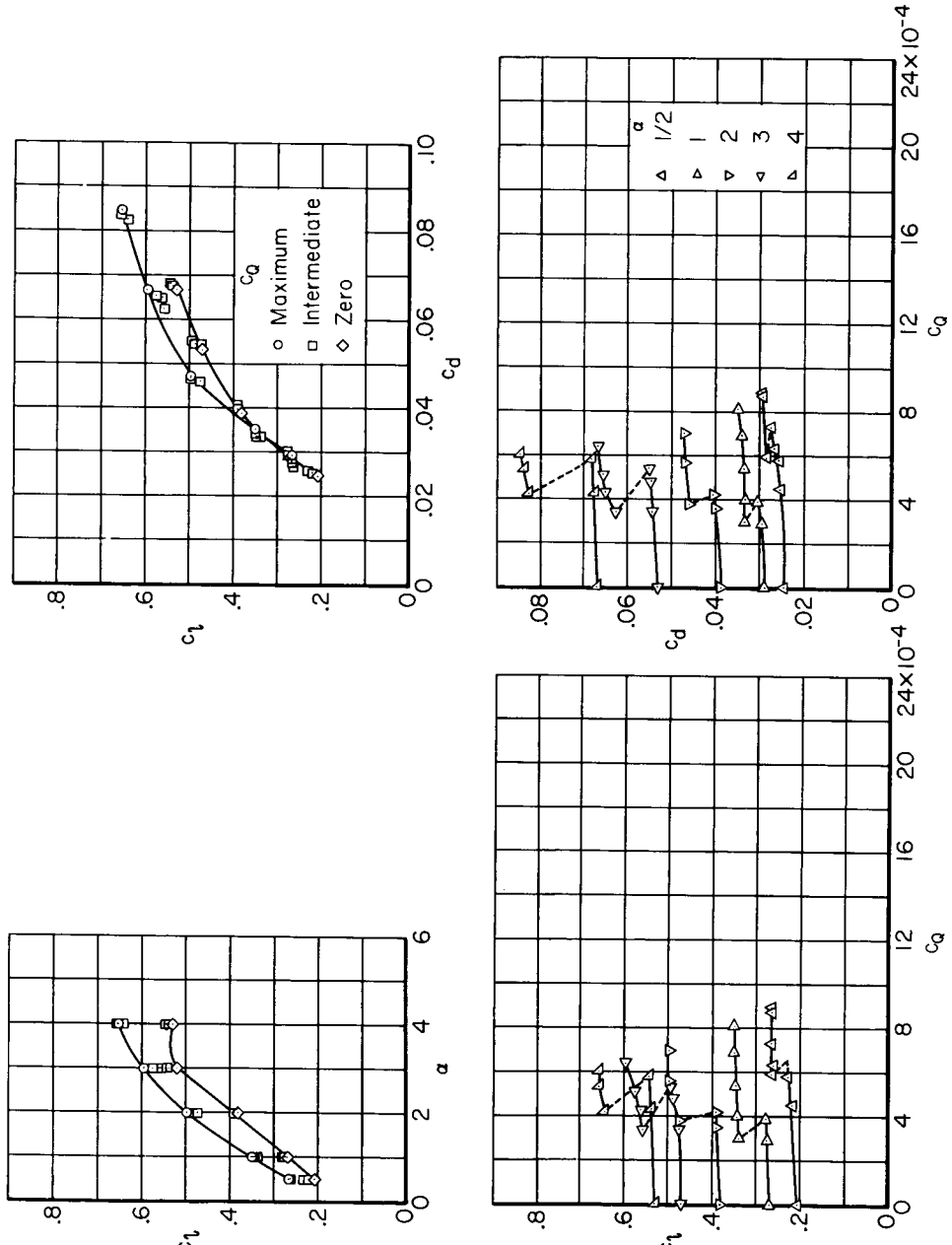

(d) $M_\infty = 0.82$

Figure 3.- Concluded.

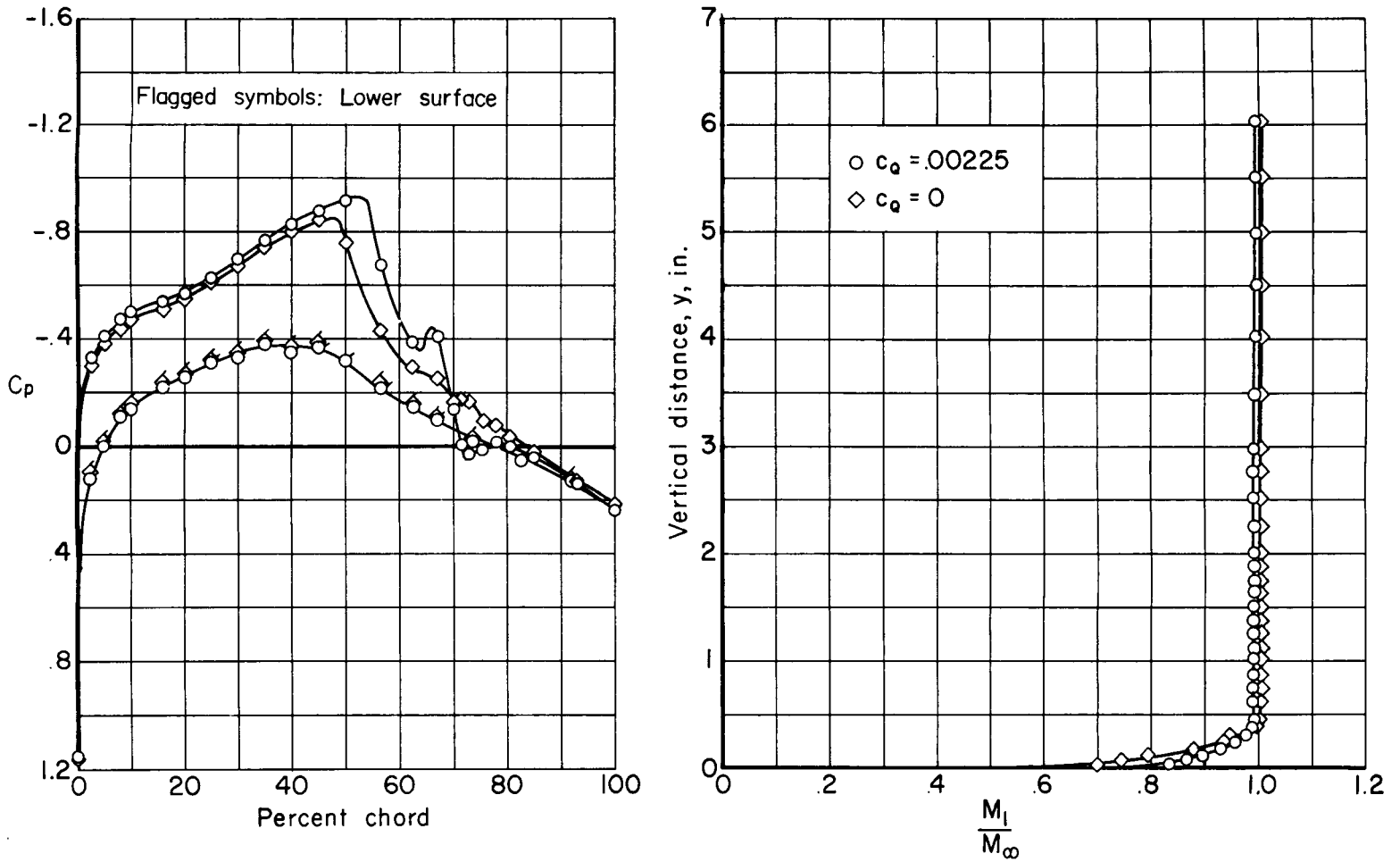

(a) $\alpha = 1/2^\circ$

Figure 4.- Effect of suction on the chordwise static-pressure distribution and on the boundary-layer profile; $M_\infty = 0.78$, $\delta = 1^\circ$, $(x/c)_{open} = 0.69$ to 0.725.

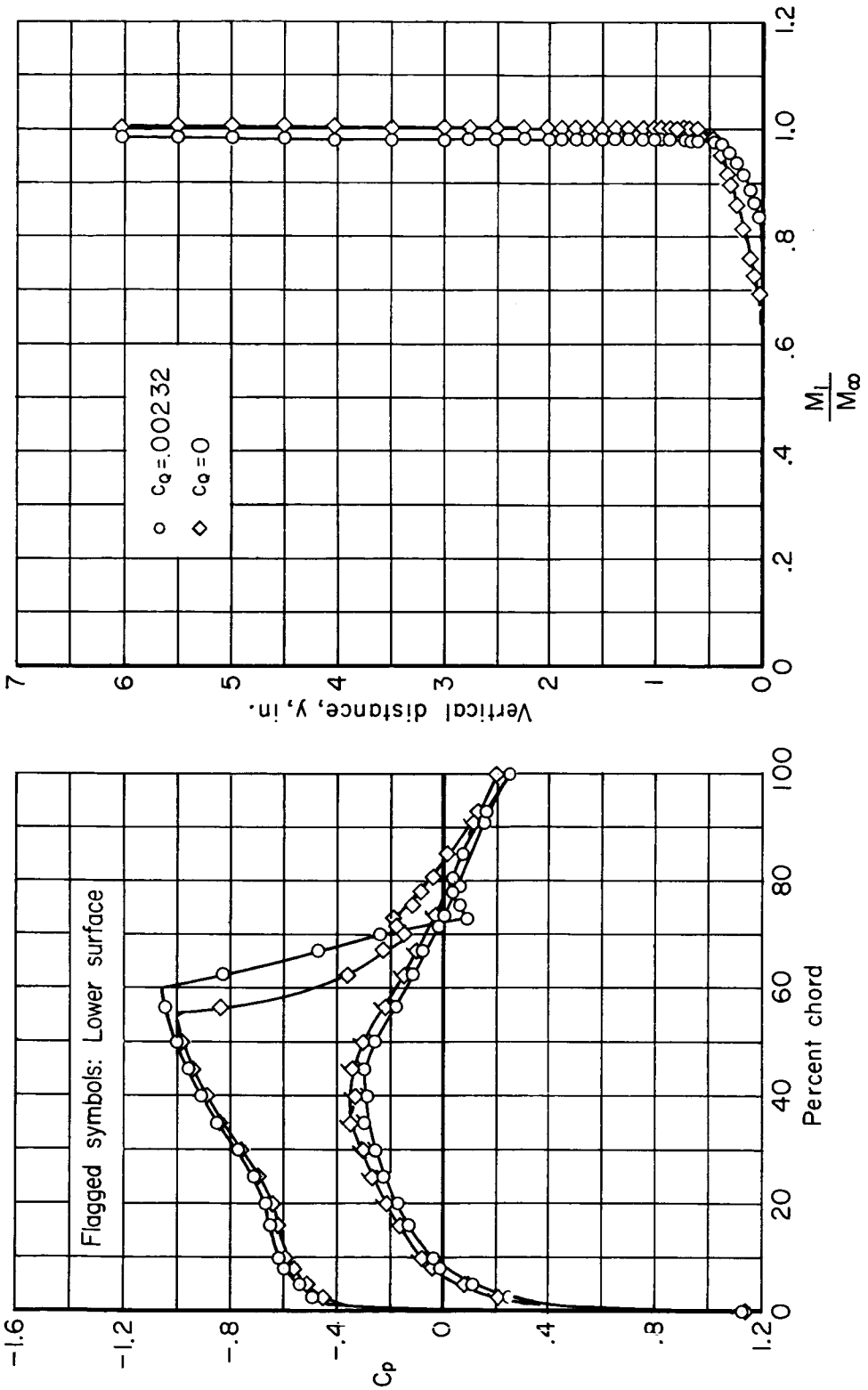

(b) $\alpha = 1^\circ$

Figure 4.- Continued.

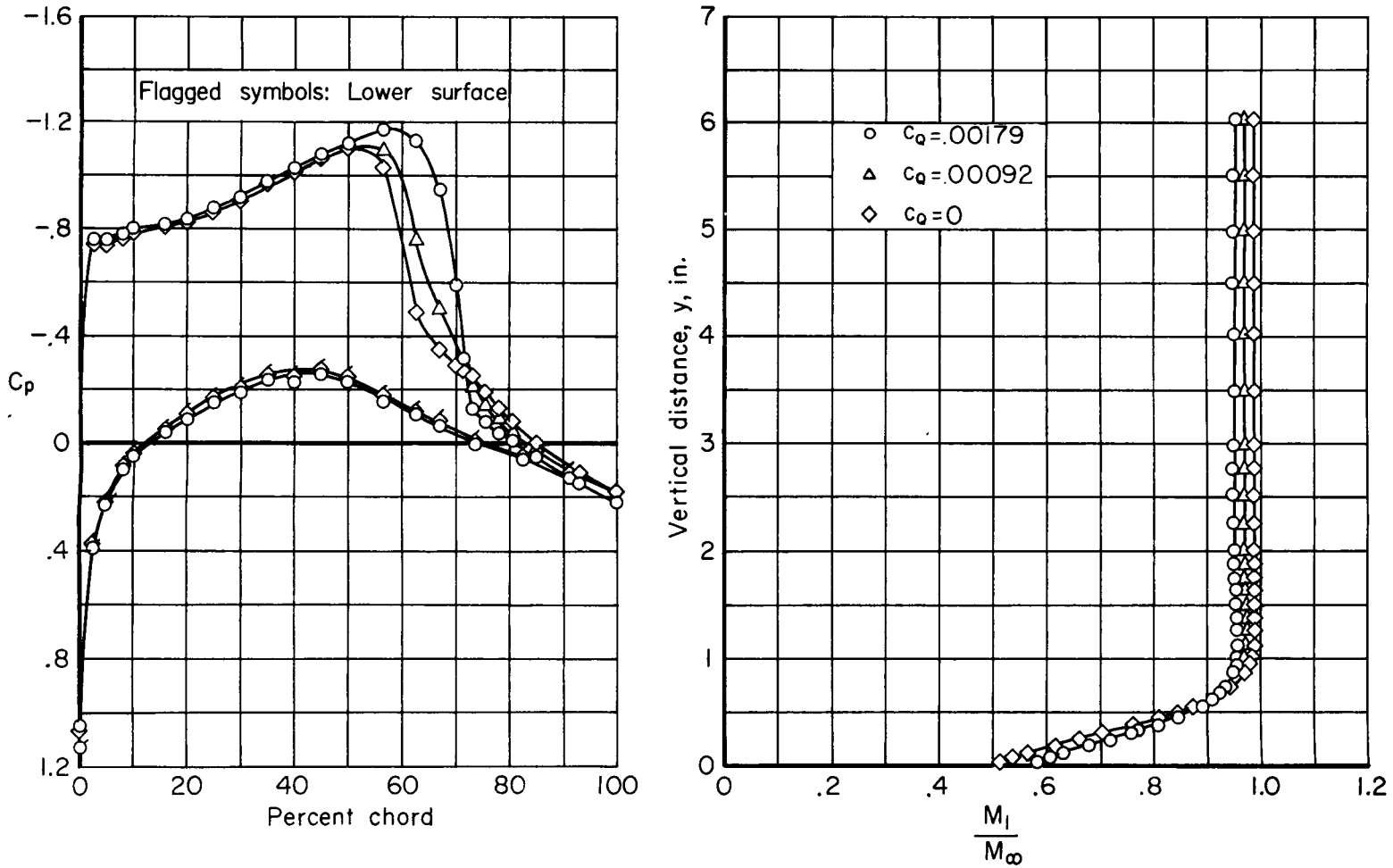

(c) $\alpha = 2^\circ$

Figure 4.- Continued.

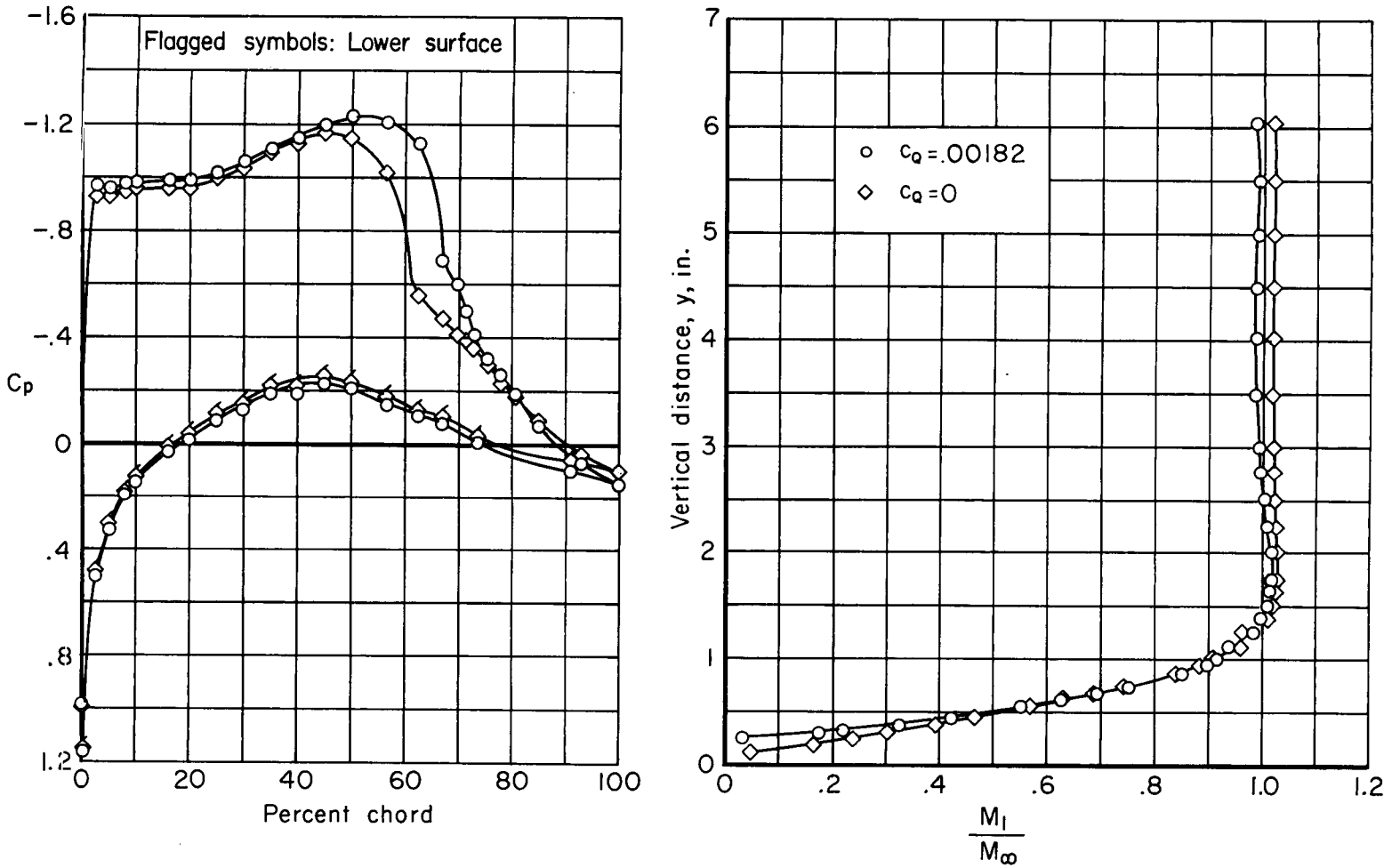

(d) $\alpha = 3^\circ$

Figure 4.- Continued.

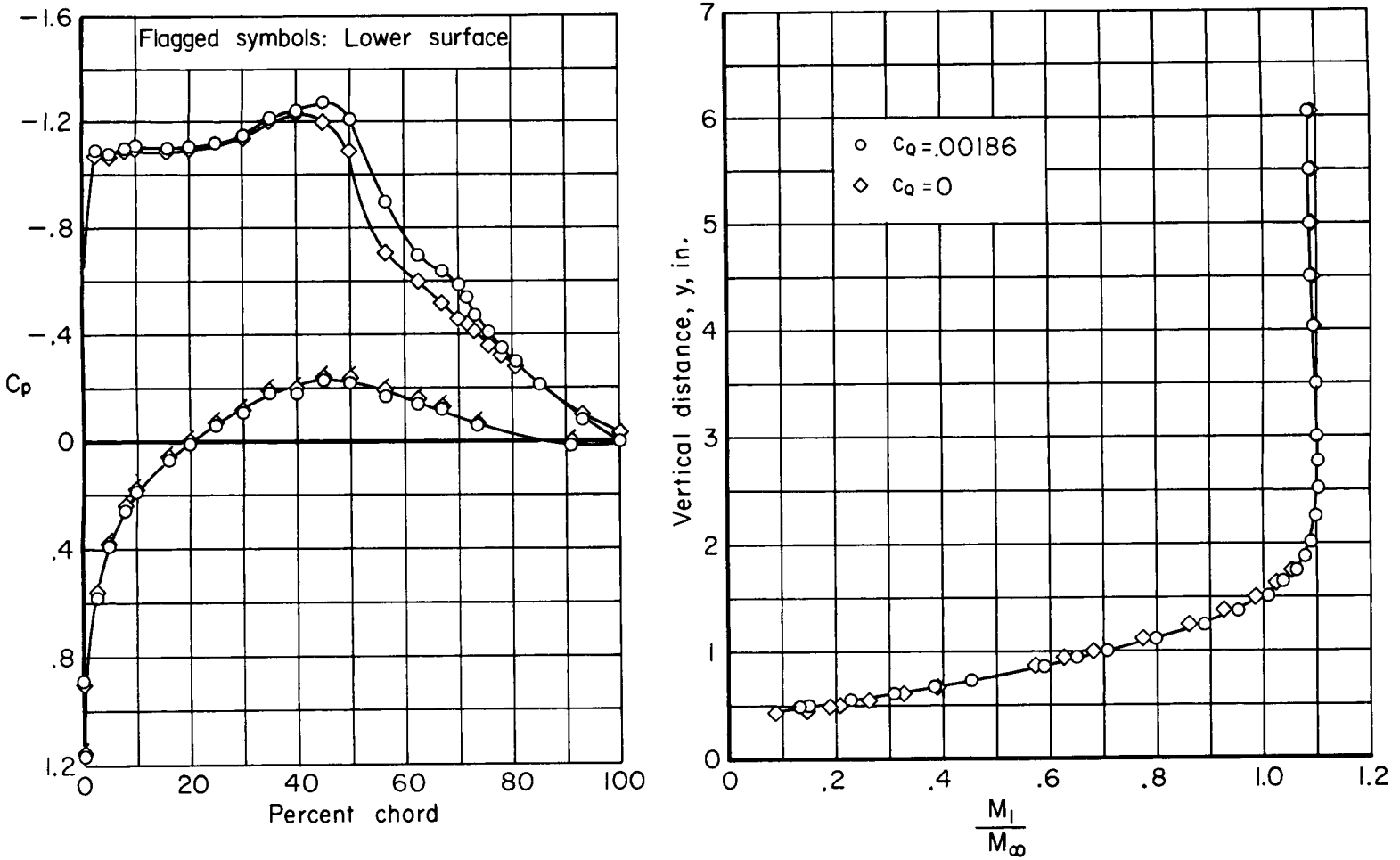

(e) $\alpha = 4^\circ$

Figure 4.- Concluded.

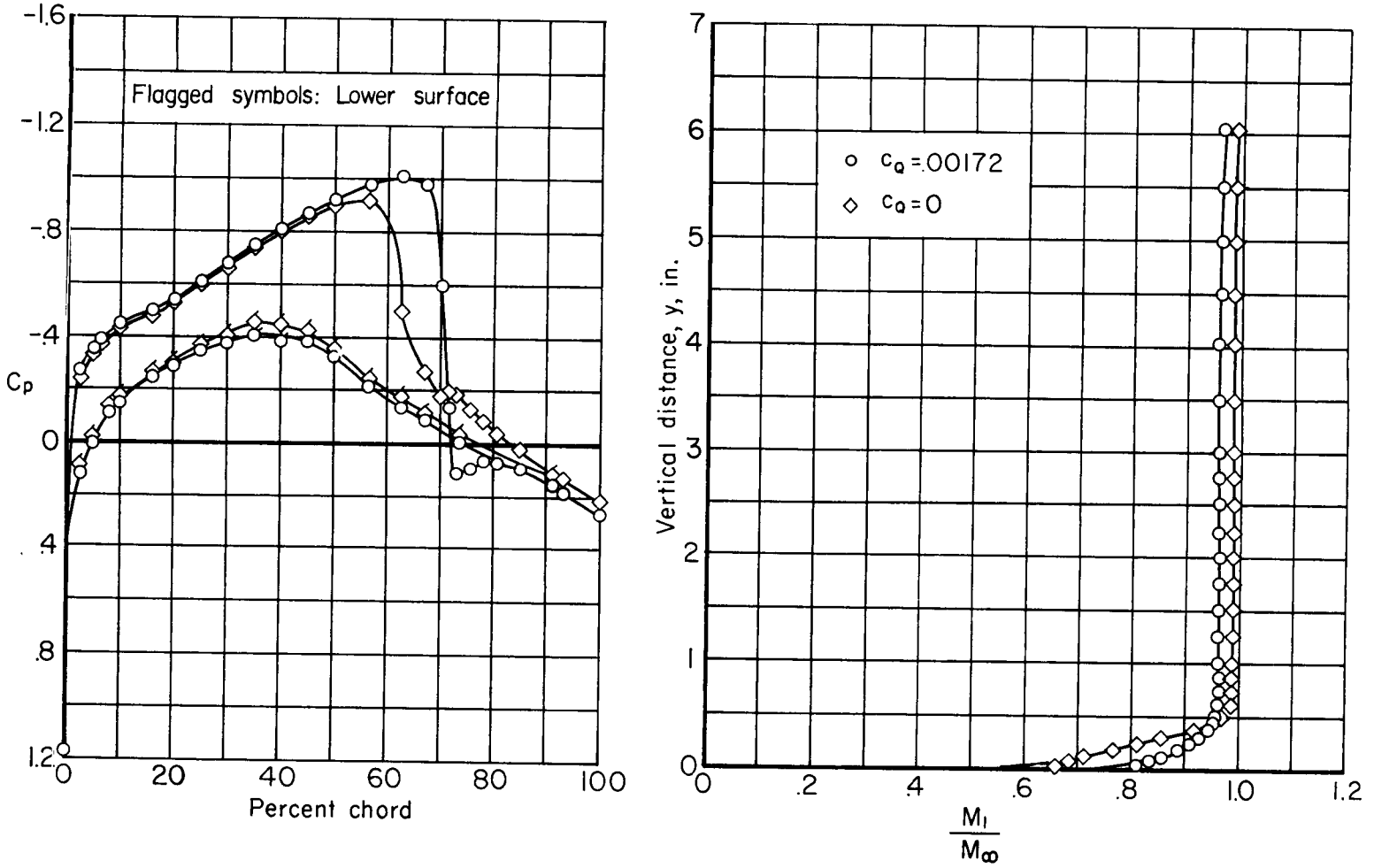

(a) $\alpha = 1/2^\circ$

Figure 5.- Effect of suction on the chordwise static-pressure distribution and on the bondary-layer profile; $M_\infty = 0.80$, $\delta = 1^\circ$, $(x/c)_{open} = 0.69$ to 0.725.

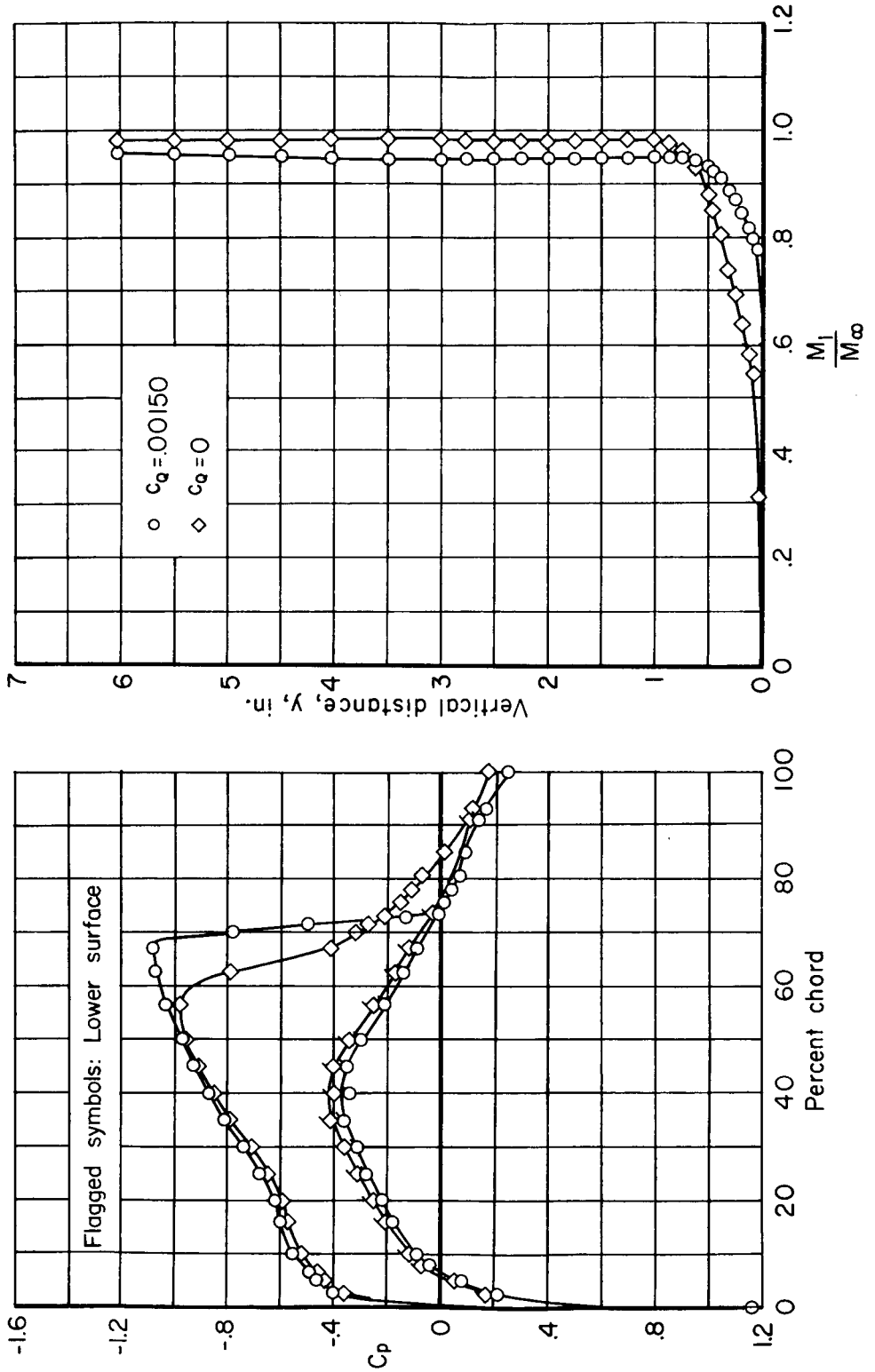

(b) $\alpha = 1^\circ$

Figure 5.- Continued.

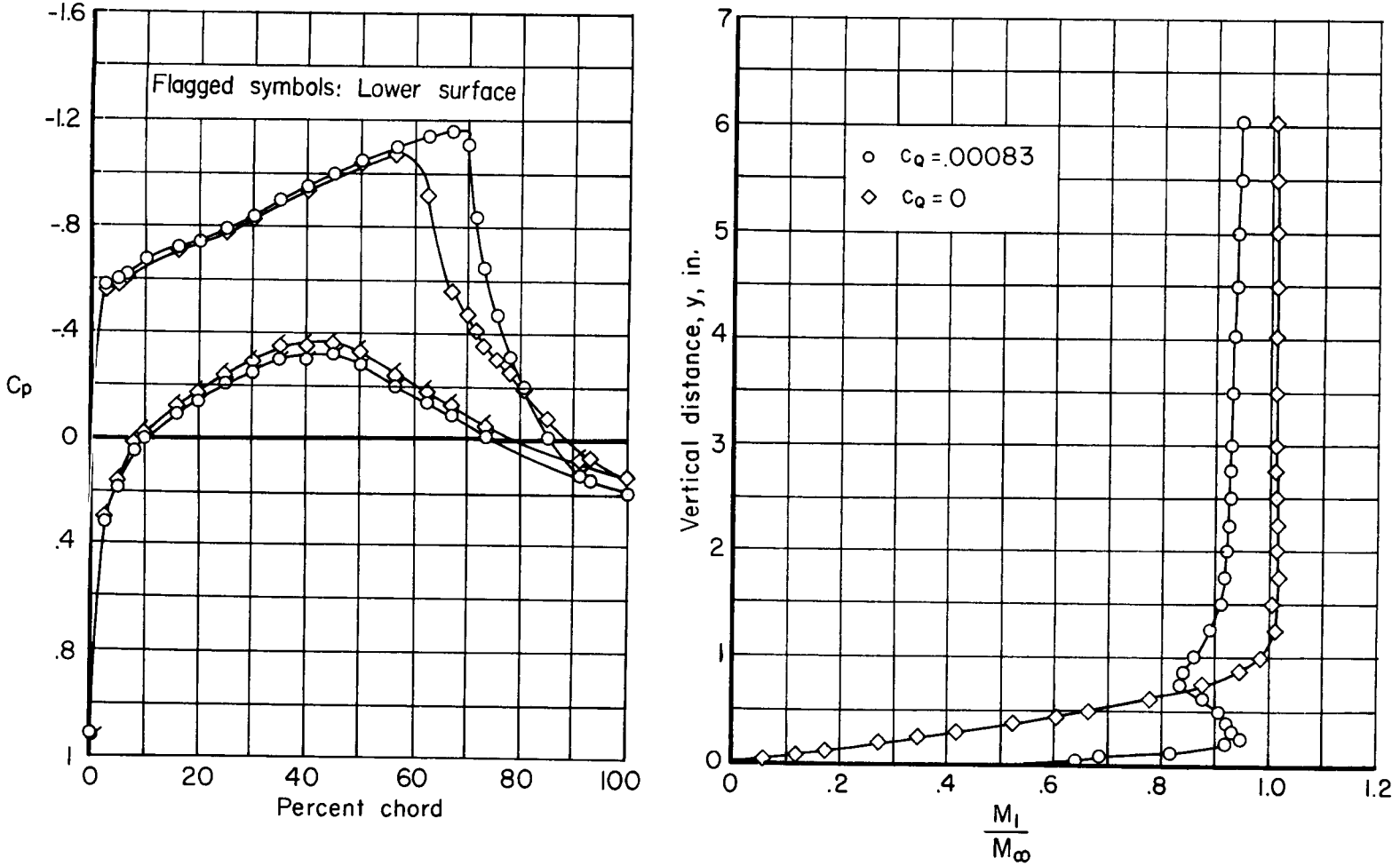

(c) $\alpha = 2^\circ$

Figure 5.- Continued.

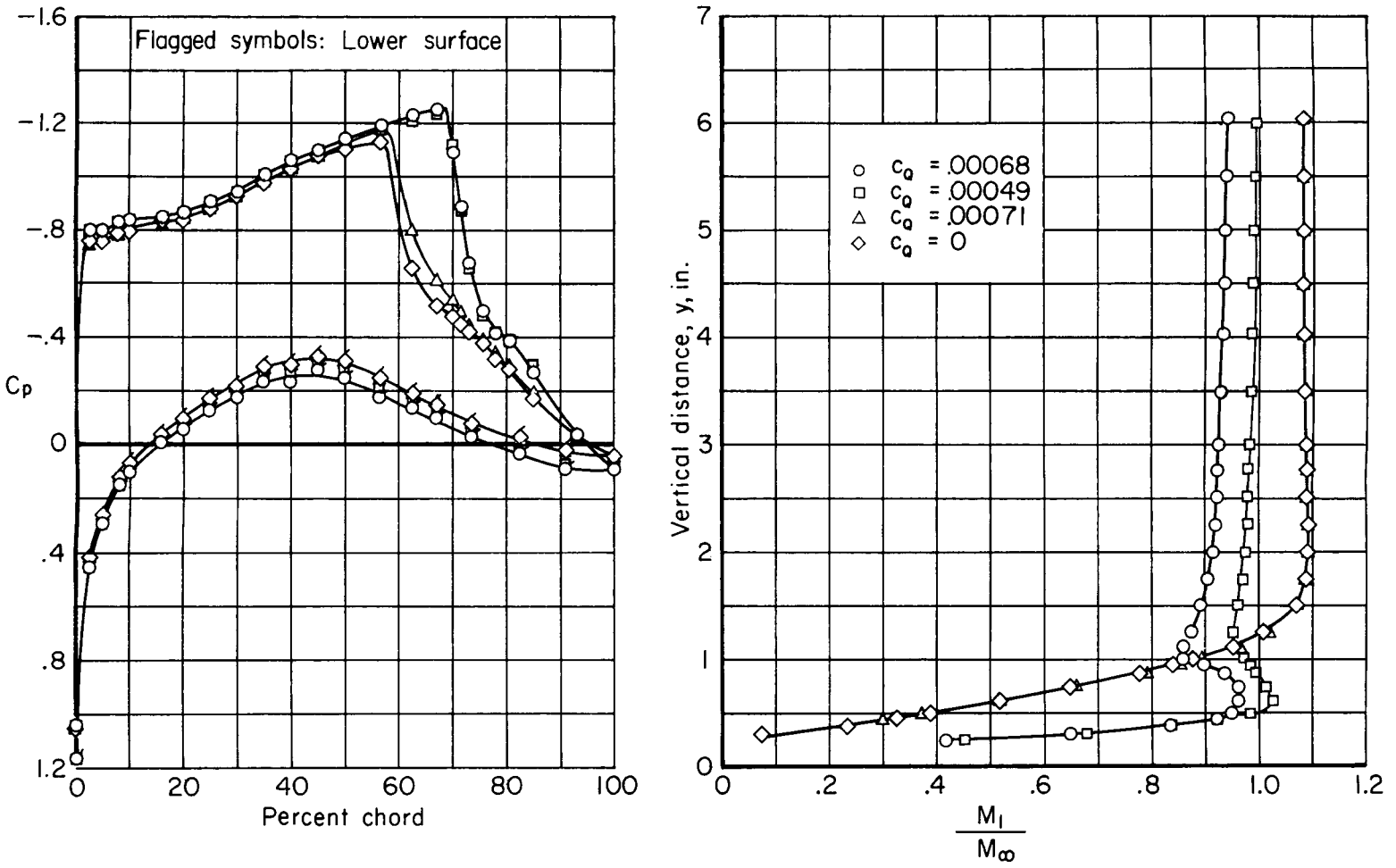

(d) $\alpha = 3^\circ$

Figure 5.- Continued.

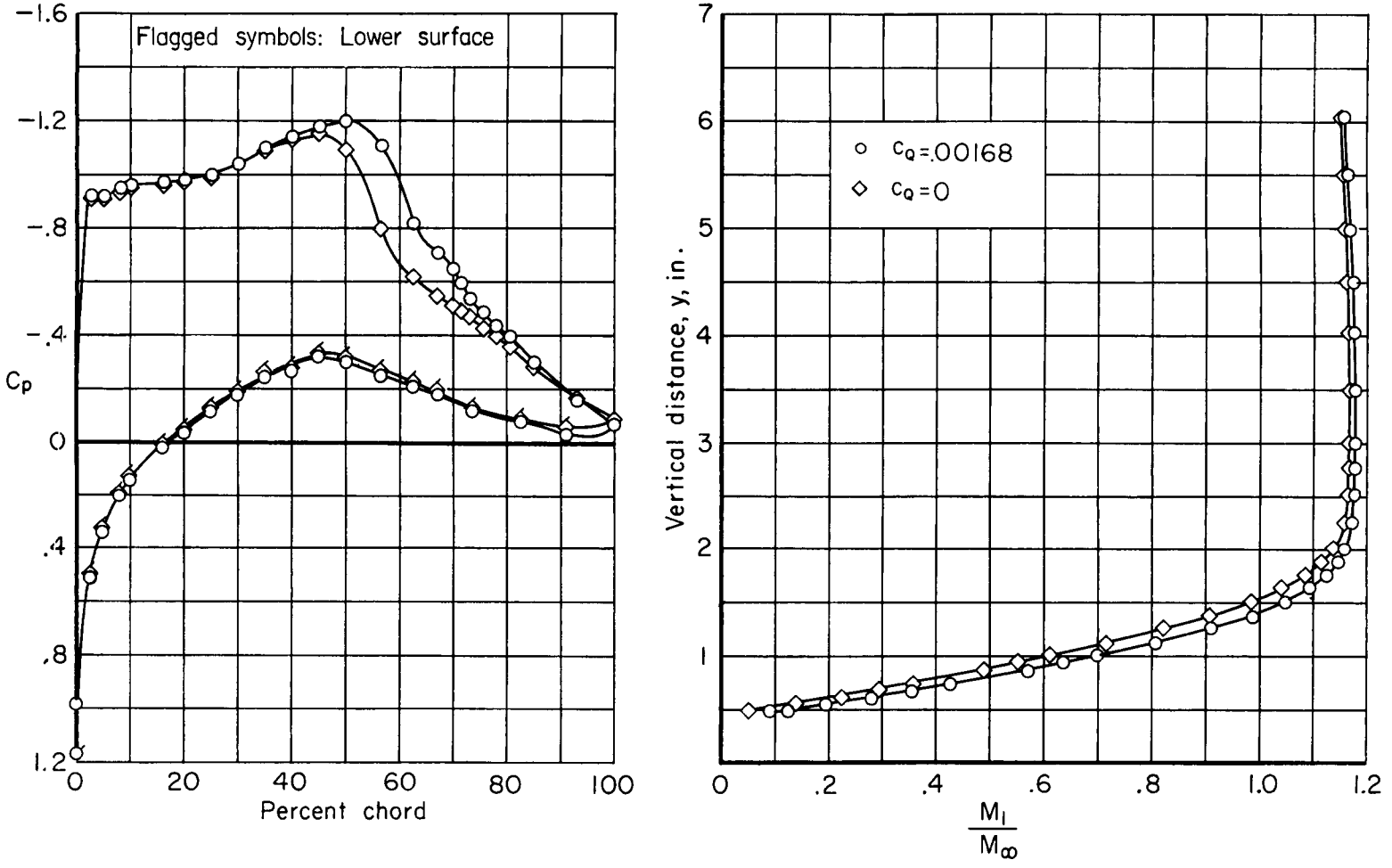

(e) $\alpha = 4^\circ$

Figure 5.- Concluded.

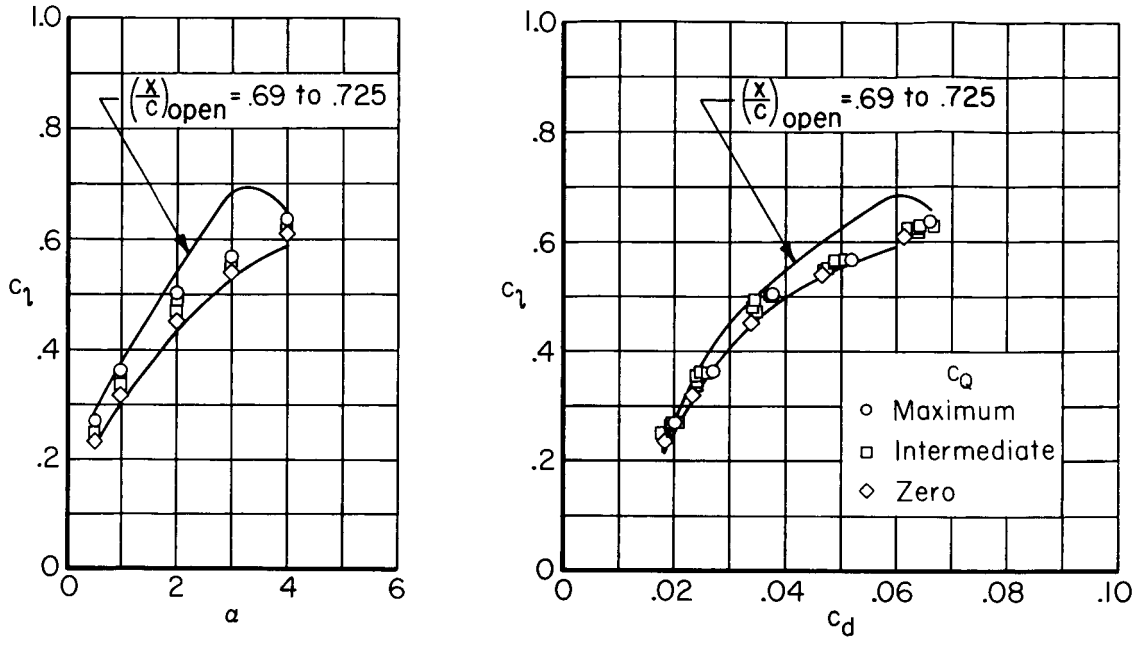

(a) $(x/c)_{open}$ = 0.69 to 0.706

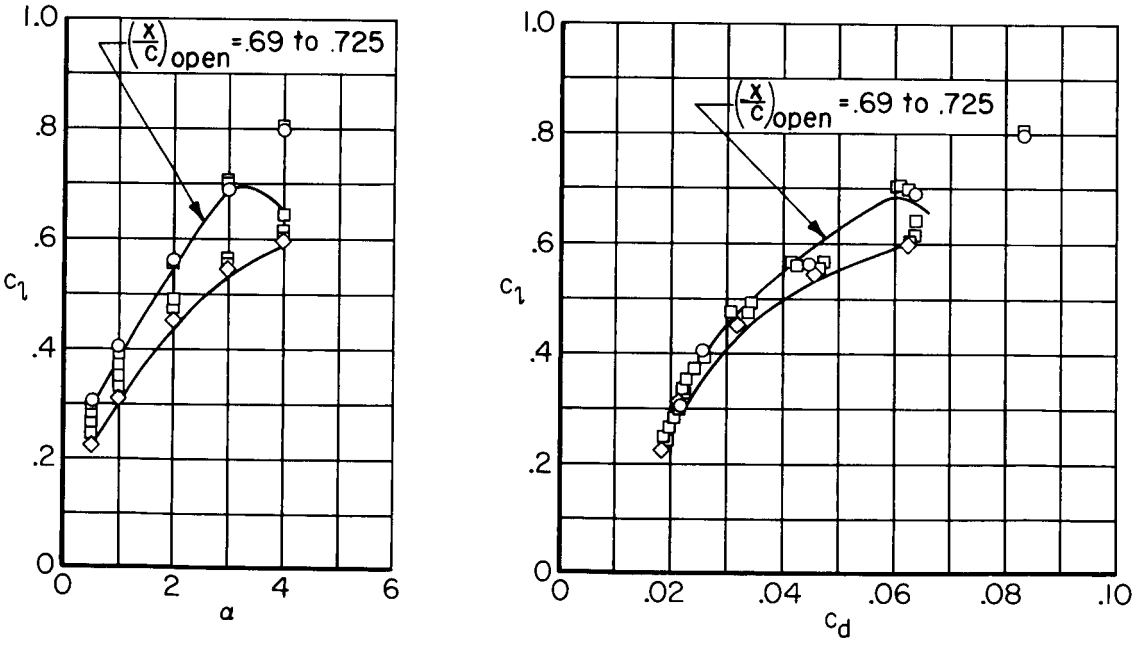

(b) $(x/c)_{open}$ = 0.69 to 0.750

Figure 6.- Effect of variation of the chordwise extent of porous area on the section lift and drag coefficient; $M_\infty = 0.80$, $\delta = 1^\circ$.

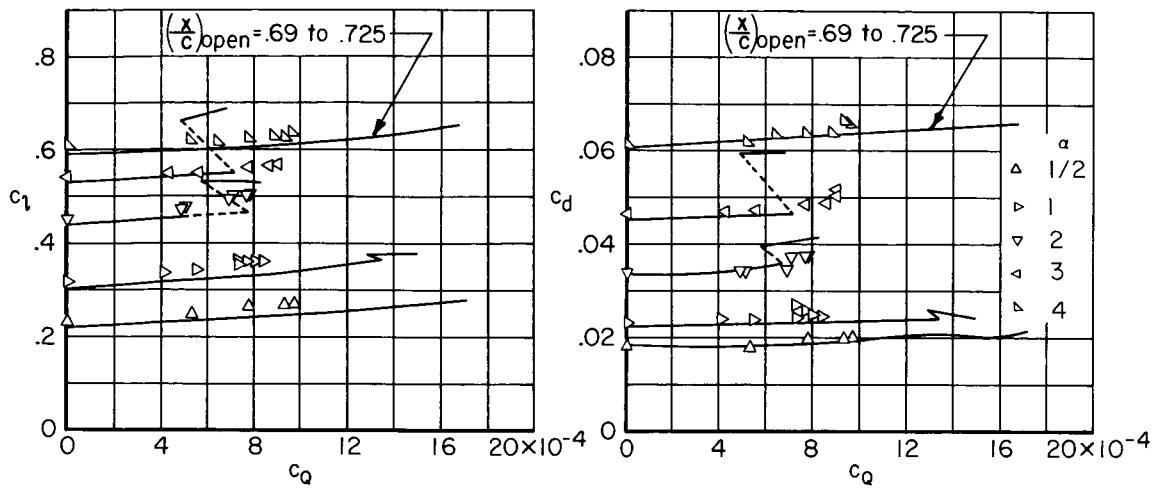

(a) $(x/c)_{open}$ = 0.69 to 0.706

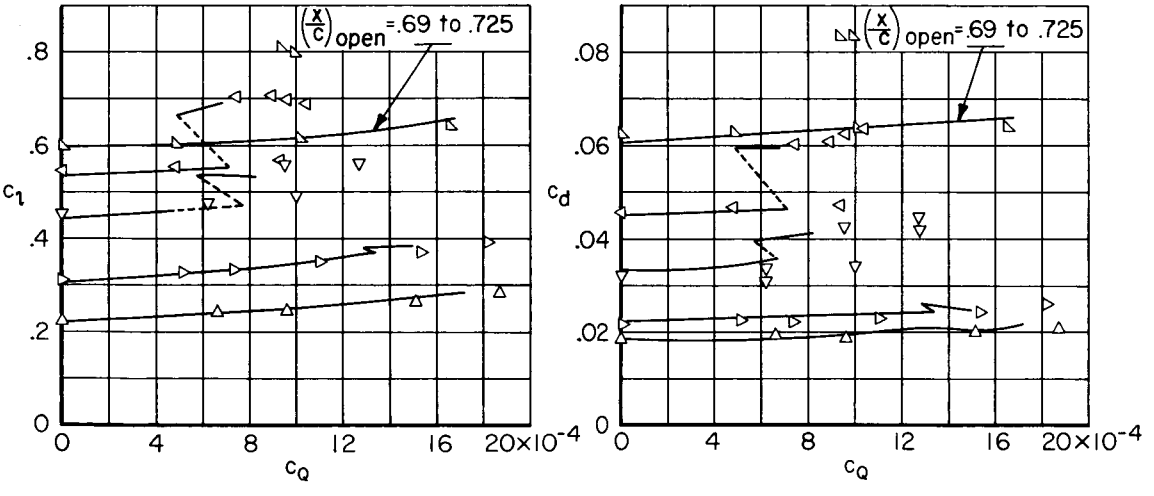

(b) $(x/c)_{open}$ = 0.69 to 0.750

Figure 7.- Effect of variation of porous area extent and suction quantity; M_∞ = 0.80, δ = 1°.

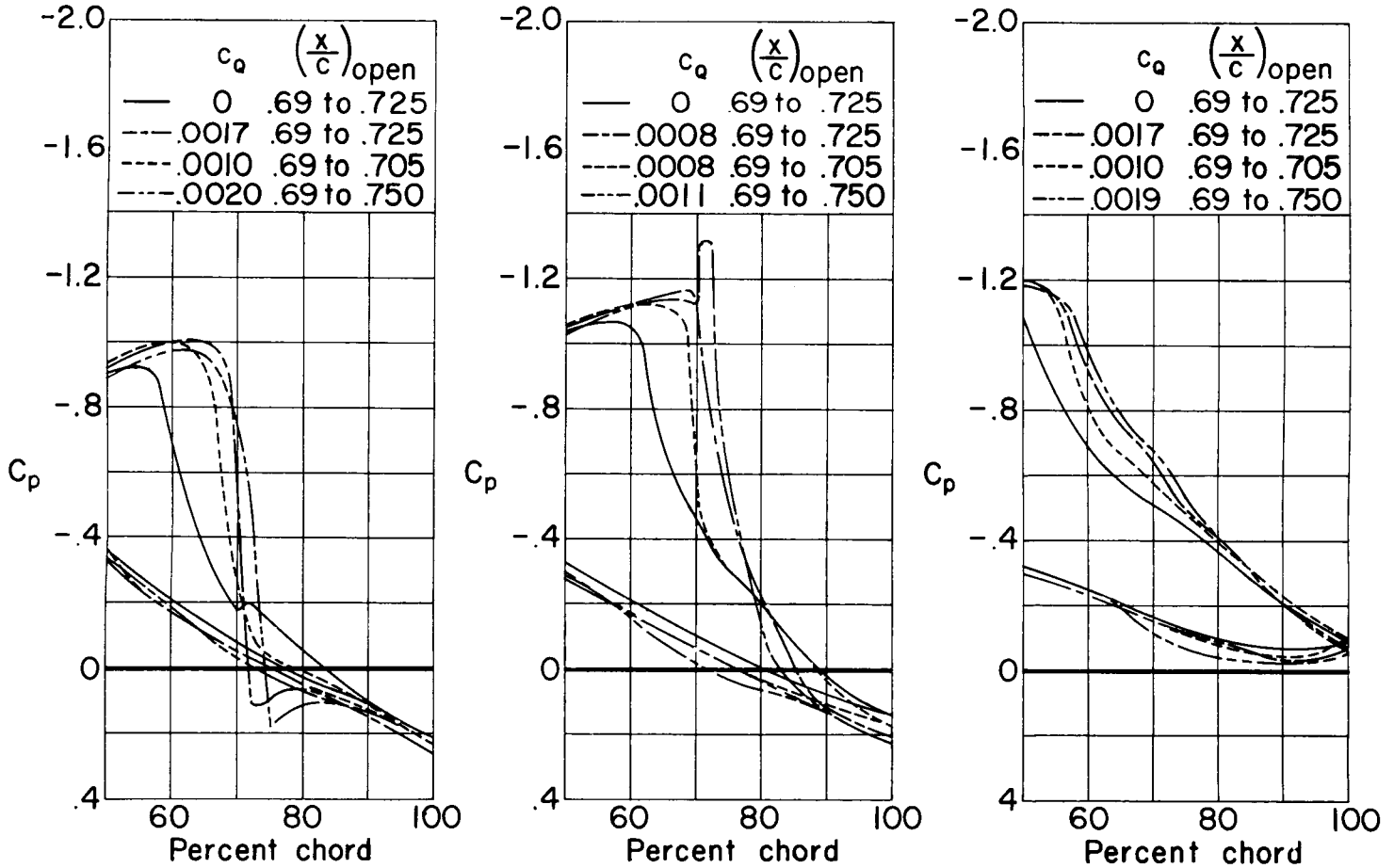

(a) $\alpha = 1/2^\circ$ (b) $\alpha = 2^\circ$ (c) $\alpha = 4^\circ$

Figure 8.- Effect of variation of the chordwise extent of porous area on the chordwise static-pressure distribution; $M_\infty = 0.80$, $\delta = 1^\circ$.

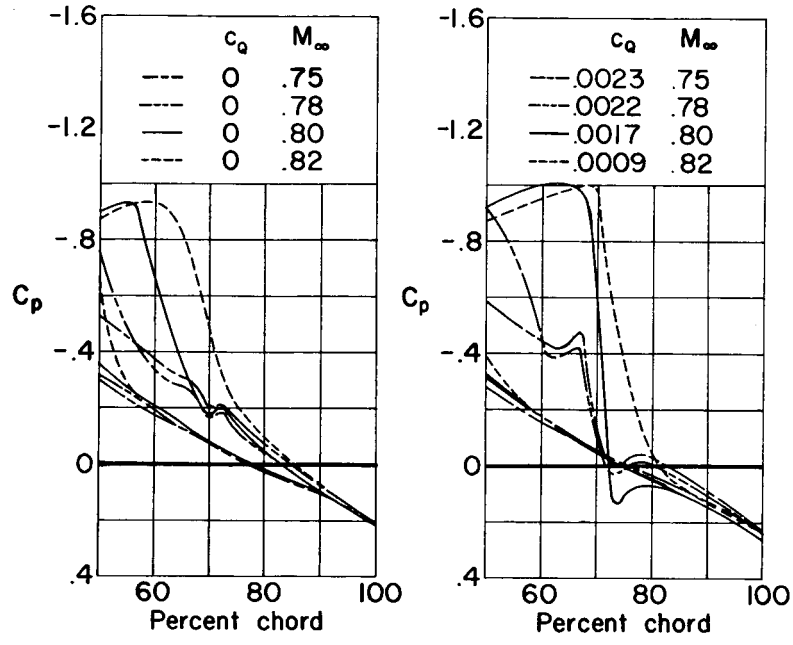

(a) $\alpha = 1/2^\circ$

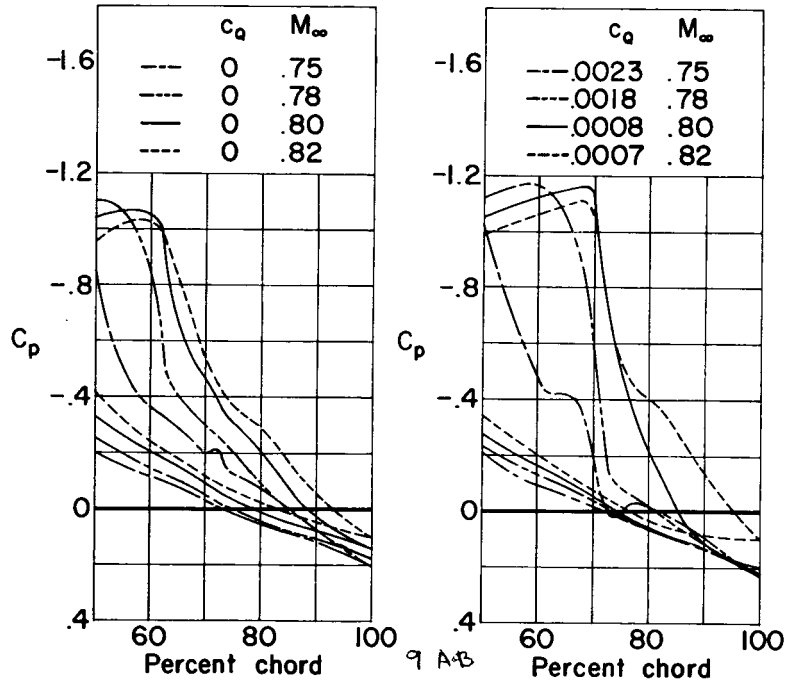

(b) $\alpha = 2^\circ$

Figure 9.- Effect of Mach number on the chordwise static-pressure distribution both with and without suction; $(x/c)_{open}$ = 0.69 to 0.725, $\delta = 1^\circ$.

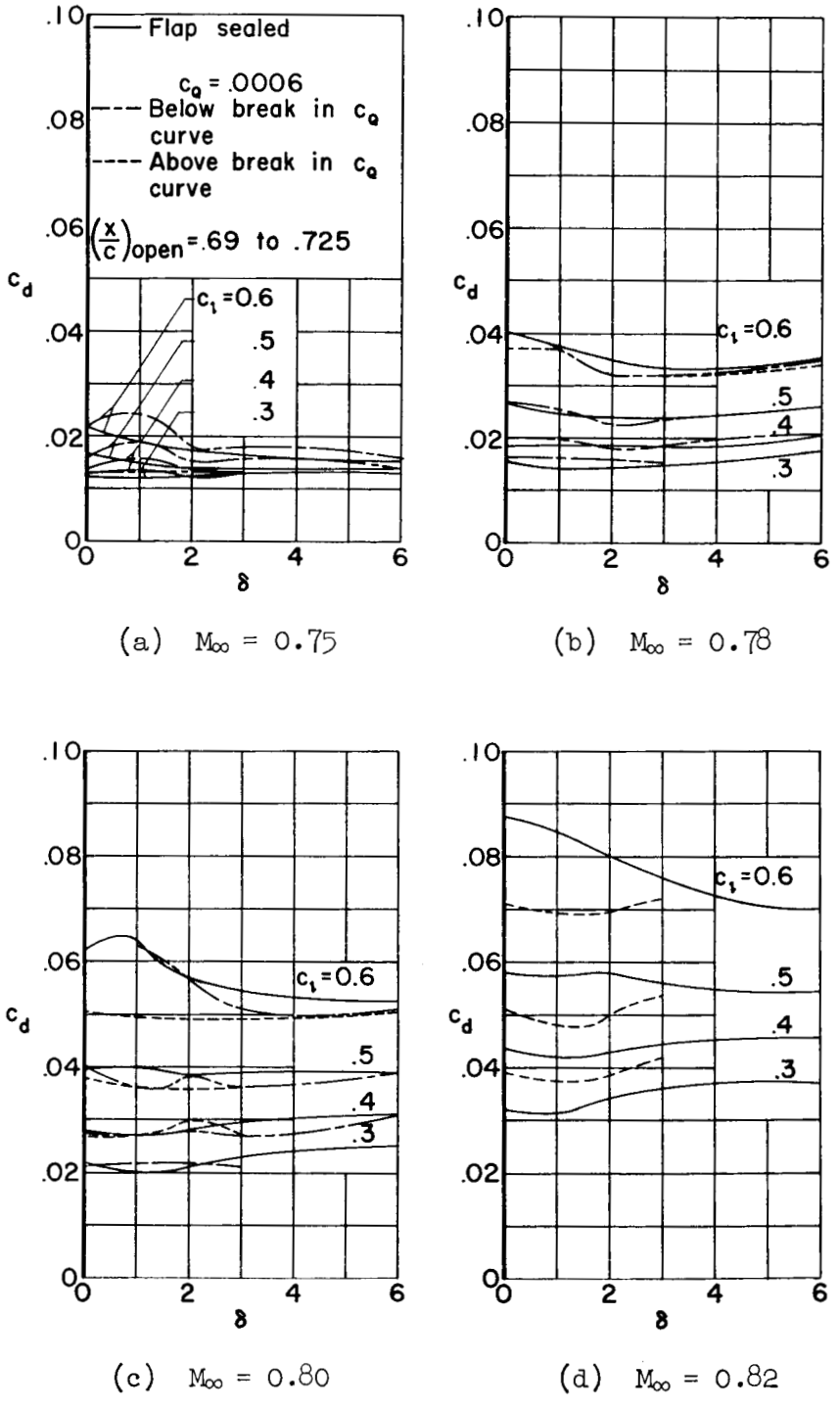

Figure 10.- Effect of suction on the variation of section drag coefficient with change in flap deflection at a constant section lift coefficient.

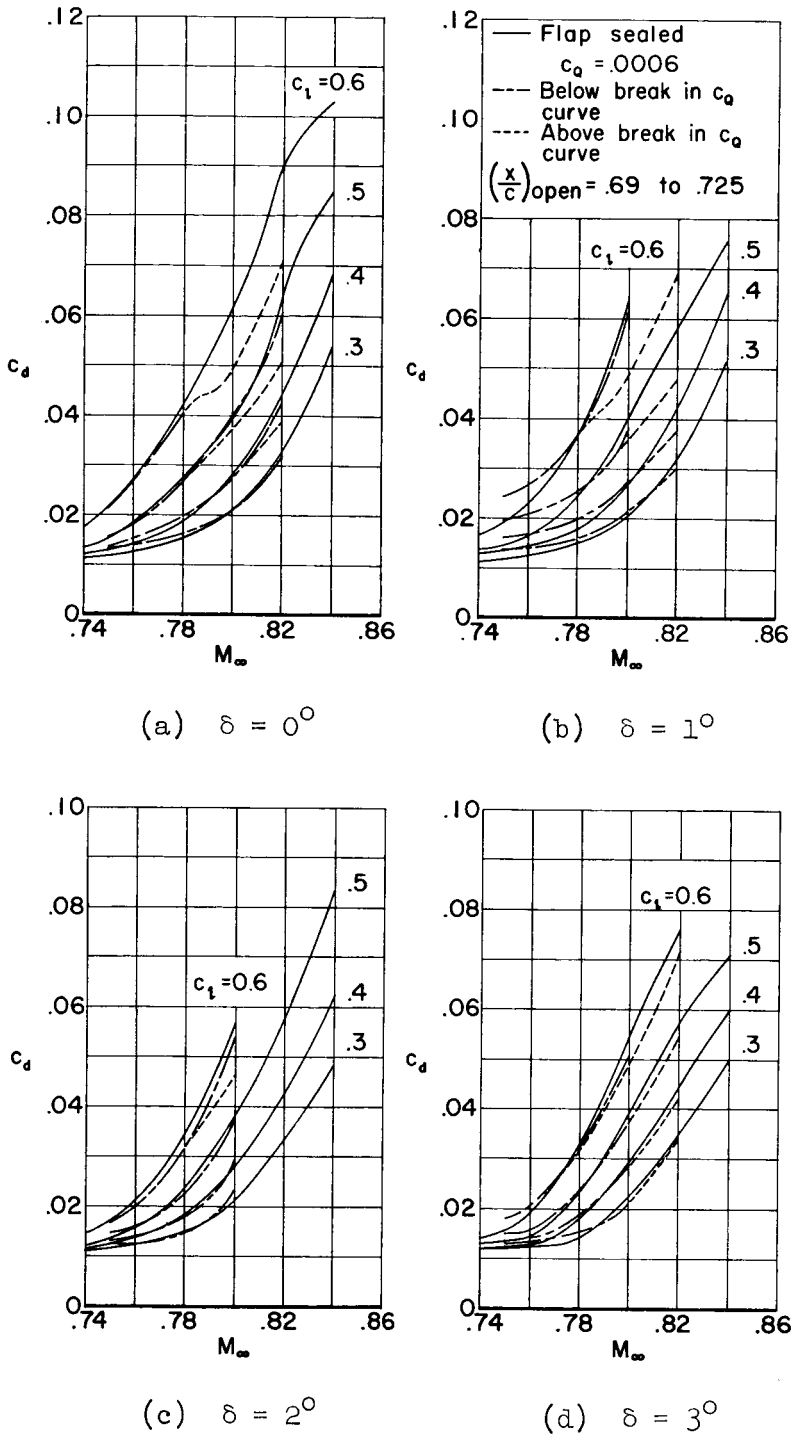

Figure 11.- Effect of suction on the variation of section drag coefficient with change in Mach number at a constant section lift coefficient.

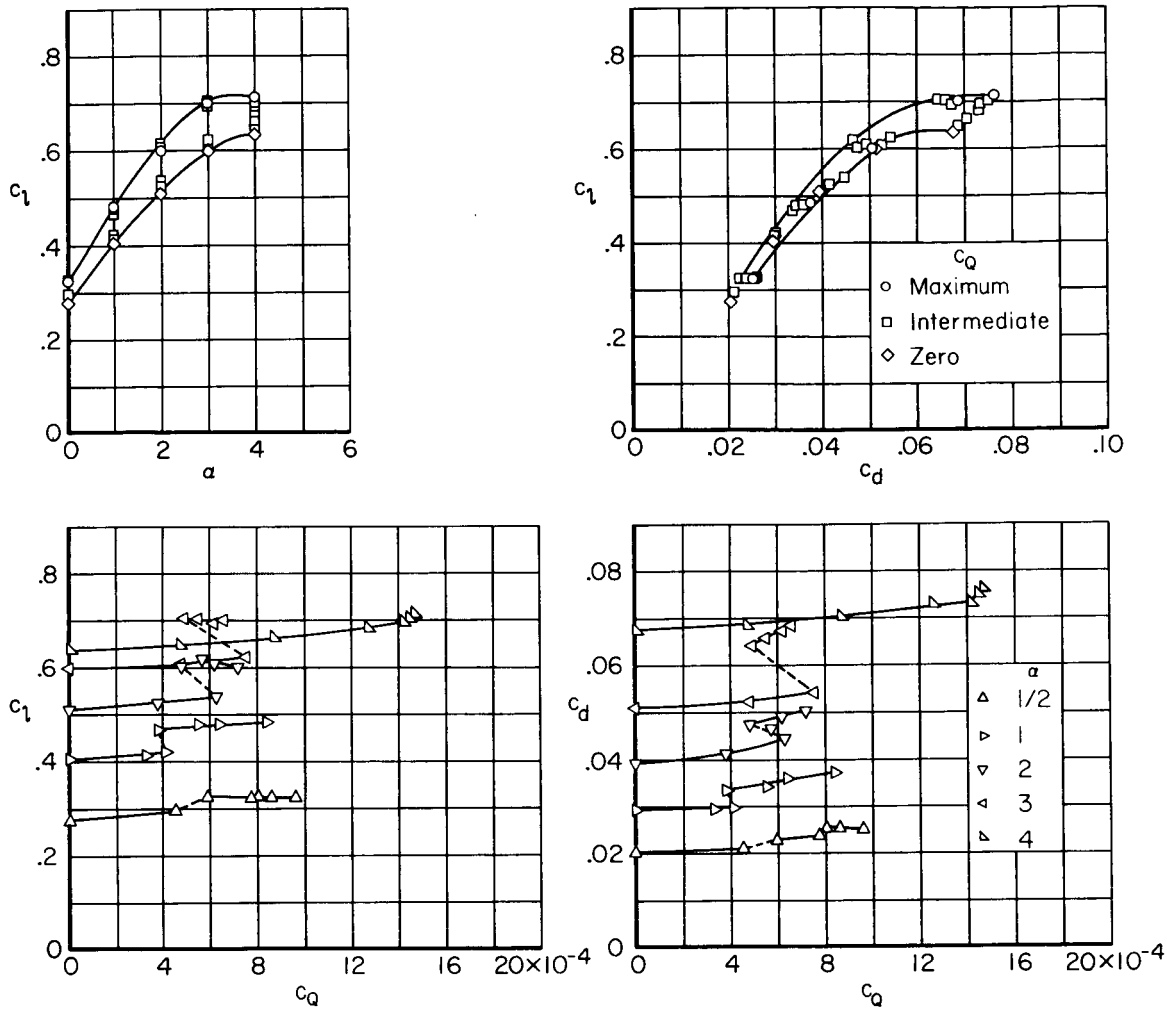

(a) Free transition.

Figure 12.- Effect of fixing transition on the section lift, drag, and suction quantity coefficients; $(x/c)_{open}$ = 0.69 to 0.725, M_∞ = 0.80, $\delta = 3^\circ$.

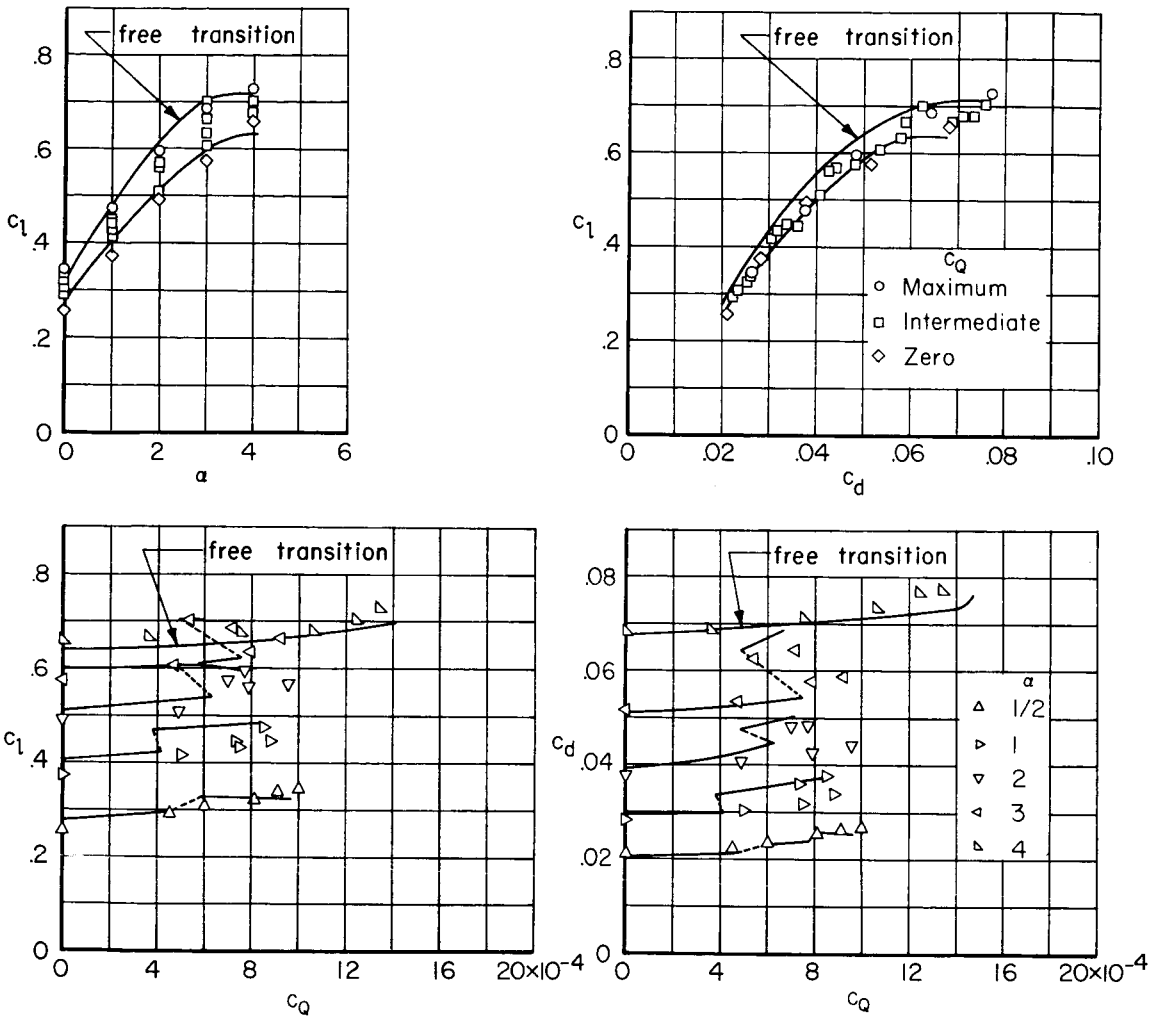

(b) 0.008-inch-diameter trip wire at x/c = 0.20.

Figure 12.- Concluded.

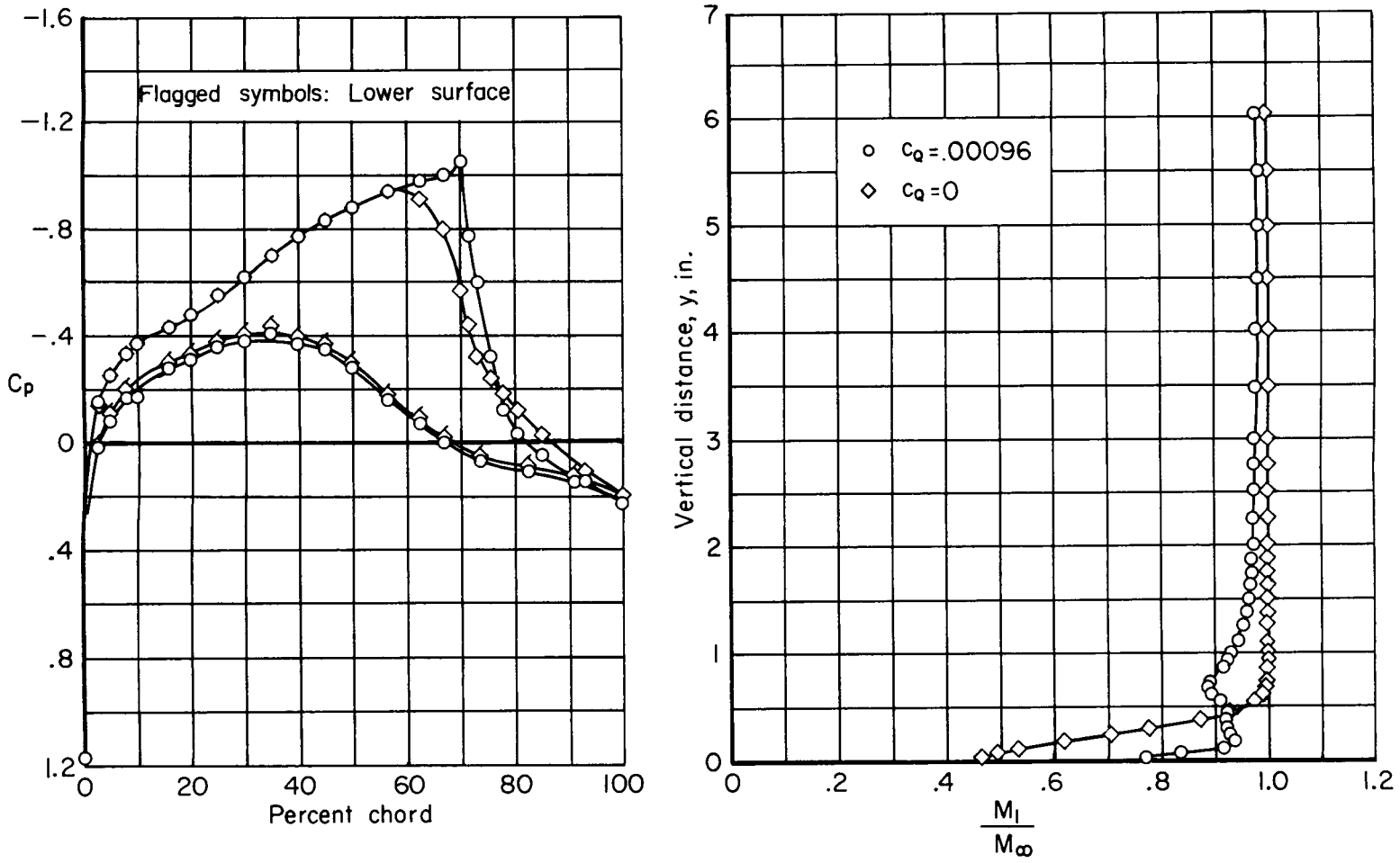

(a) $\alpha = 0^\circ$

Figure 13.- Effect of suction on the chordwise static-pressure distribution and on the boundary-layer velocity profile; $M_\infty = 0.80$, $\delta = 3^\circ$, $(x/c)_{open} = 0.69$ to 0.725, free transition.

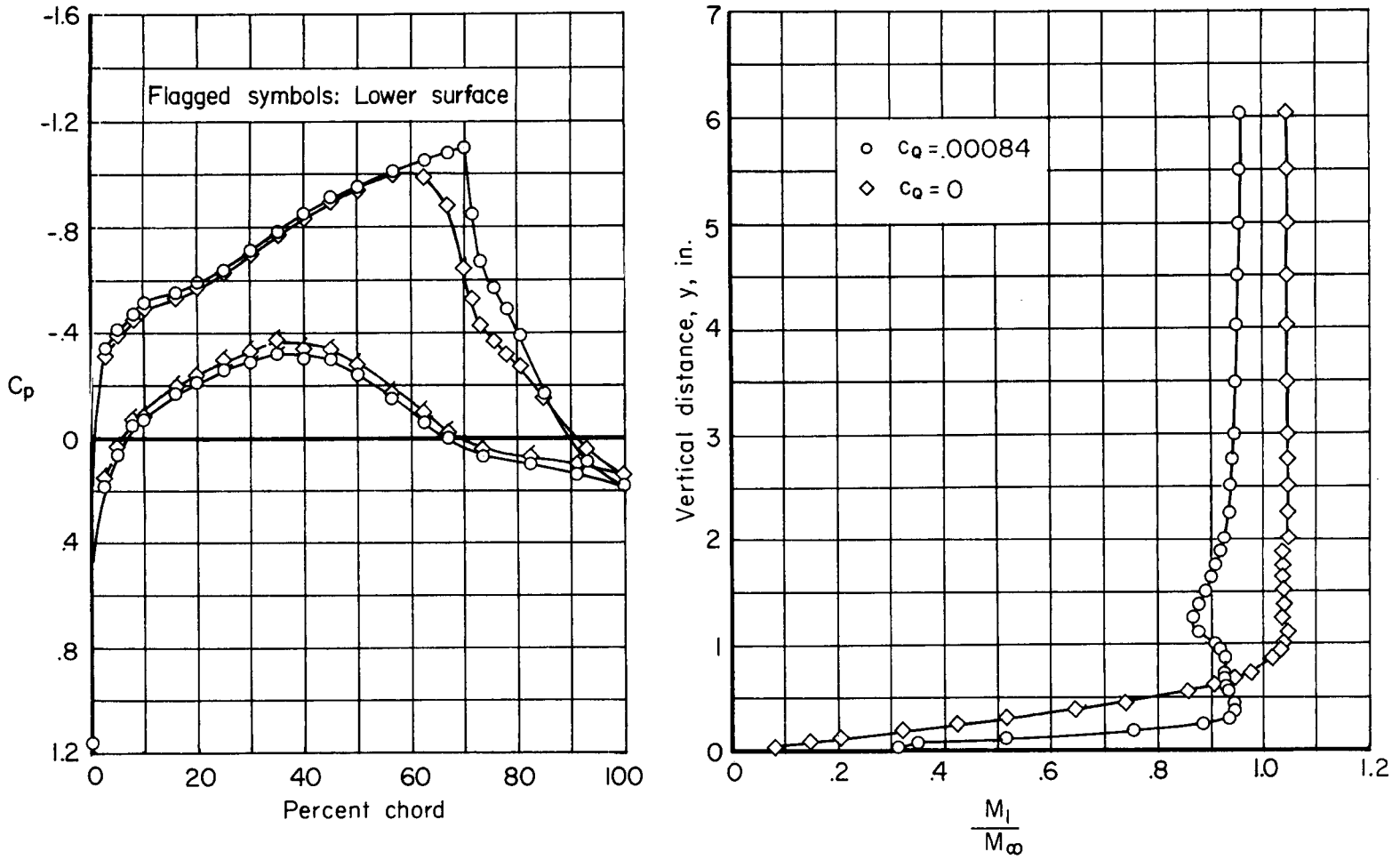

(b) $\alpha = 1^\circ$

Figure 13.- Continued.

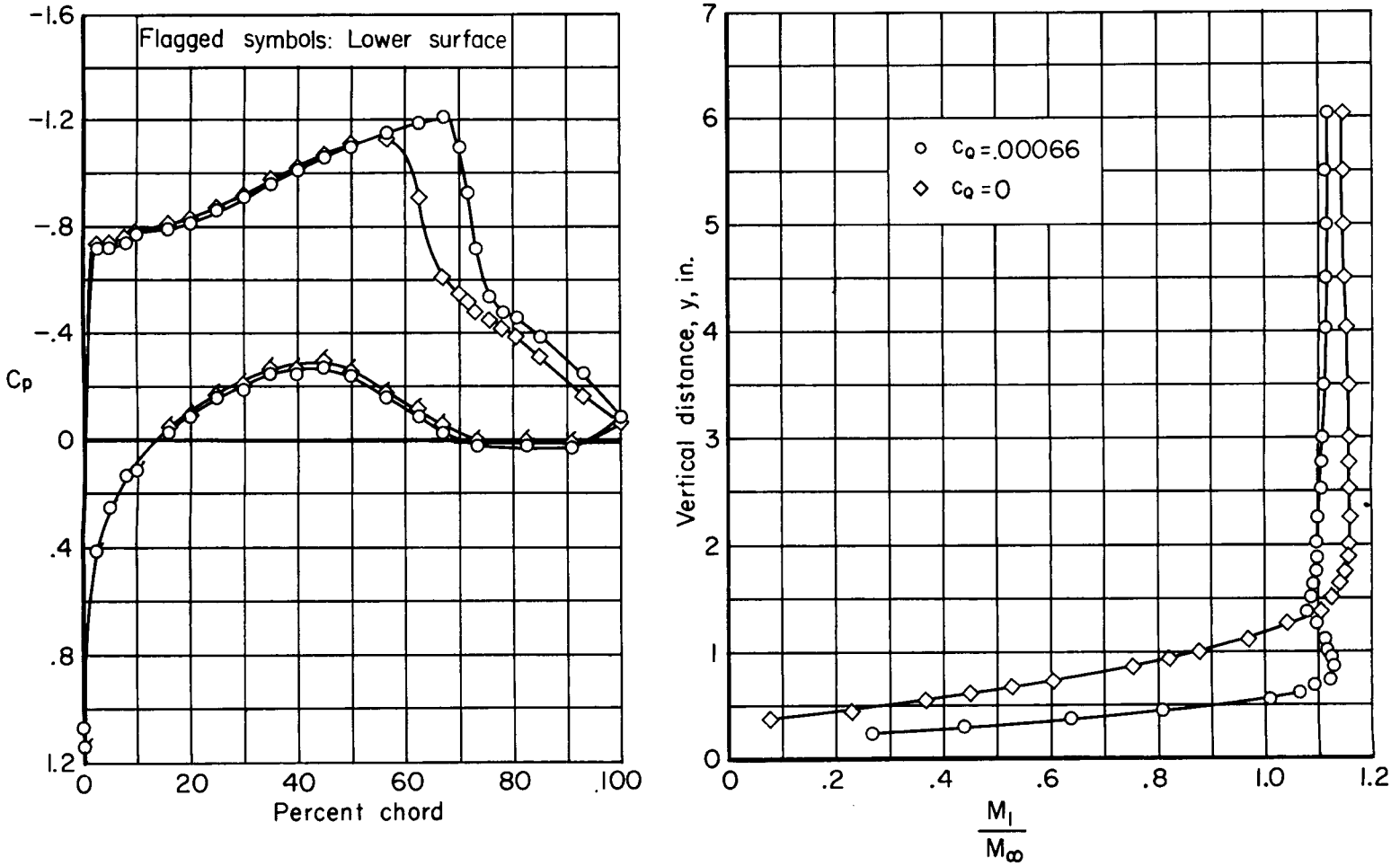

(c) $\alpha = 3^\circ$

Figure 13.- Concluded.

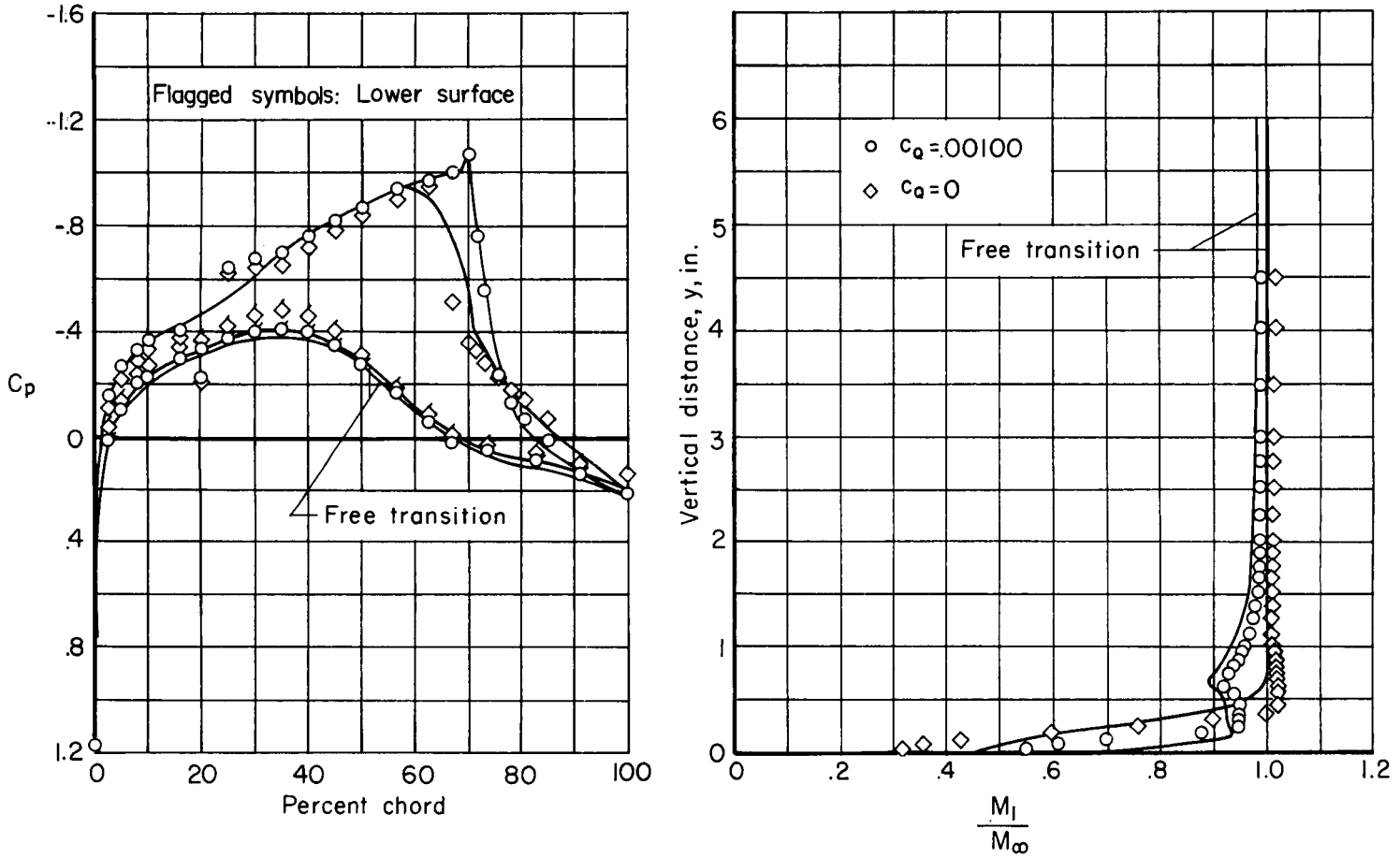

(a) $\alpha = 0^\circ$

Figure 14.- Effect of fixing transition on the chordwise static pressure distribution and on the boundary layer velocity profile; $M_\infty = 0.80$, $\delta = 3^\circ$, $(x/c)_{open} = 0.69$ to 0.725, 0.008-inch-diameter trip wire at $x/c = 0.20$.

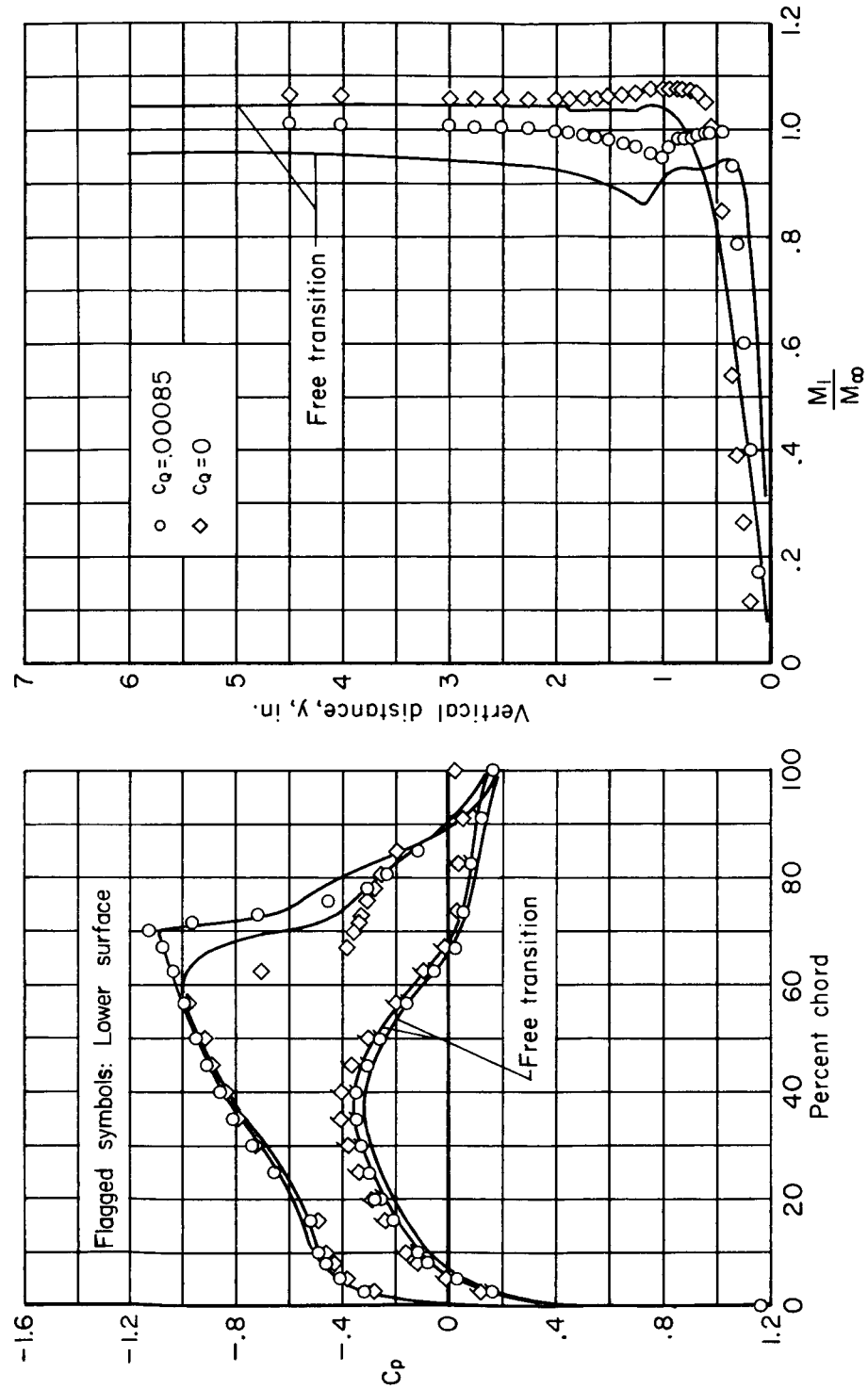

(b) $\alpha = 1^\circ$

Figure 14.- Continued.

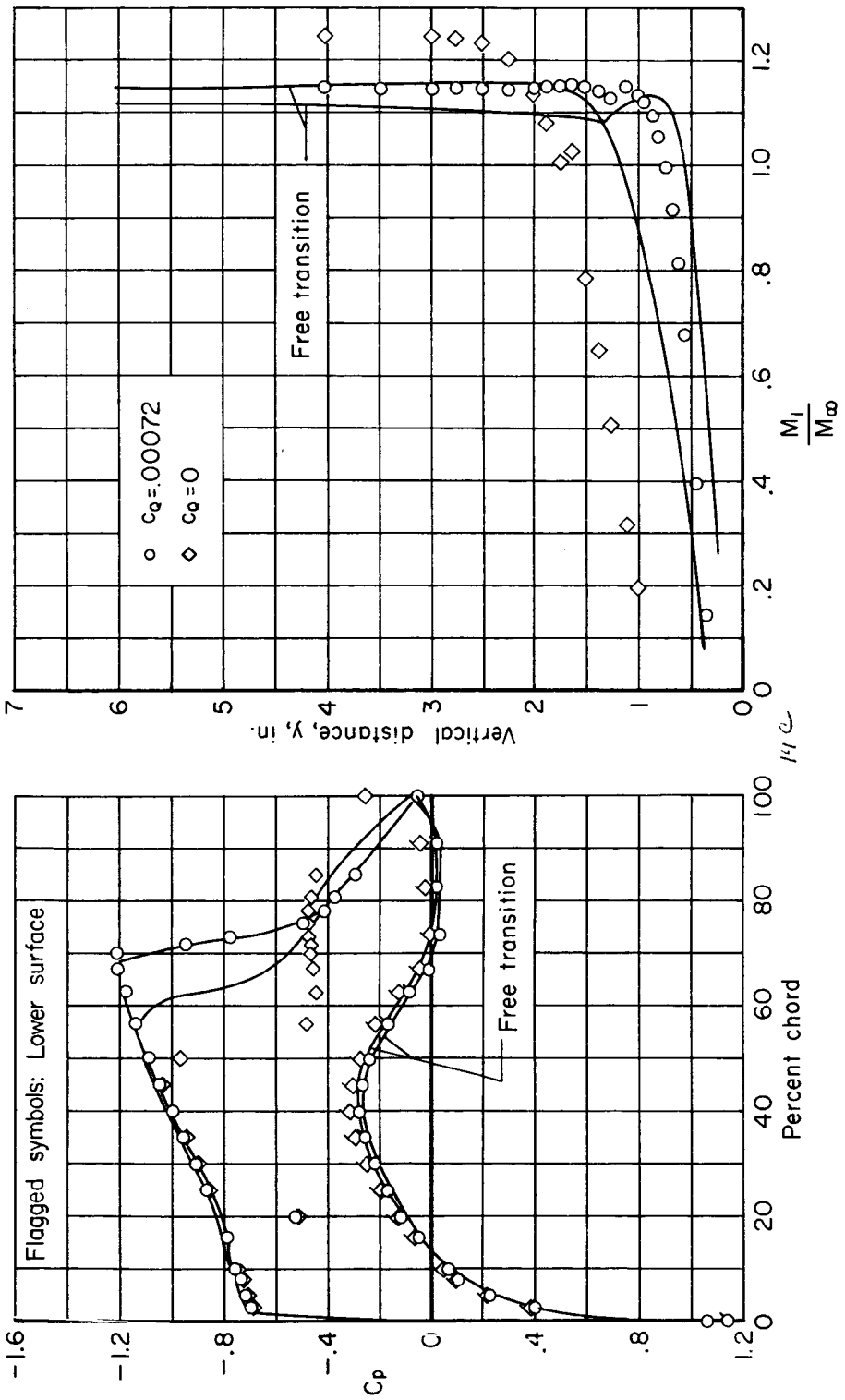

(c) $\alpha = 3^\circ$

Figure 14.- Concluded.